FATİH UNIVERSITY

The Institute Of Bionano Technology

**Master of Science in
Bio And Nano Technology Engineering**

NANO MATERIAL DOPED ORGANIC SOLAR CELL PRODUCTION AND CHARACTERIZATION

by

Yasin ARSLAN

November 2015

NANO MATERIAL DOPED ORGANIC SOLAR CELL PRODUCTION AND CHARACTERIZATION

by

Yasin ARSLAN

A thesis submitted to

the Institute Of Bionano Technology

of

Fatih University

in partial fulfillment of the requirements for the degree of

Master of Science

in

Bio and Nano Technology Engineering

November 2015
Istanbul, Turkey

APPROVAL PAGE

This is to certify that I have read this thesis written by Yasin ARSLAN and that in my opinion it is fully adequate, in scope and quality, as a thesis for the degree of Master of Science in Bio and Nano Technology Engineering.

_____
Asst. Prof.Yakup BAKIŞ
Thesis Supervisor

I certify that this thesis satisfies all the requirements as a thesis for the degree of Master of Science in Bio and Nano Technology Engineering.

_____
Prof. Ayhan BOZKURT
Head of Department

Examining Committee Members

Prof. Rauf SÜLEYMANLI   _____

Asst. Prof.Yakup BAKIŞ   _____

Asst. Prof Hüseyin SAĞKOL   _____

It is approved that this thesis has been written in compliance with the formatting rules laid down by the Graduate School of Bio and Nano Technology Engineering.

_____
Prof. Ayhan BOZKURT
Director

November 2015

NANO MATERIAL DOPED ORGANIC SOLAR CELL PRODUCTION AND CHARACTERIZATION

Yasin ARSLAN

M.S. Thesis – Bio and Nano Technology Engineering
November 2015

Thesis Supervisor: Asst. Prof. Yakup BAKIŞ

ABSTRACT

Researches about organic solar cell (OSC) have been accelerated in recent 15 years. Developments and new inventions about polymer science in parallel contributed significantly to the amount of investigations about OSC. Easy production processes, and diversity, low design costs, and applicable to various surfaces are remarkable features of OSCs'. The range of Polymers which used in OSCs is wide and they can be manipulated via noncomplex chemical processes and possible to obtain desired photoelectrical, physical and chemical characteristics. In this thesis Bulk heterojunction OSC s have been studied. Firstly a ITO-PEDOT:PSS-P3HT/PCBM-Al structure produced in standard efficiency. Sample preparation procedures, coating methods and working conditions, layer thicknesses, have been optimized. Structural layer specifications have been monitored via Atomic Force Microscopy,(AFM), Scanning Electron Microscopy and Fluoro spectroscopy analyzing methods. Secondly, Gold Nano particles have been doped between anode and cathode layers of OSC and solar conversion efficiencies have been investigated. Lastly Short Circuits, Current densities, Open circuit Voltages, Filling factors and solar energy conversions have been measured.

Keywords:Organic Solar Cell, ITO, Conductive Polymers, Bulk Heterojunction

NANO MALZEME KATKILI ORGANİK GÜNEŞ HÜCRESİ ÜRETİMİ VE KARAKTERİZASYONU

Yasin ARSLAN

Yüksek Lisans Tezi – Biyo ve Nano Teknoloji Mühendisliği
Kasım 2015

Tez Danışmanı Yard.Doc.Dr. Yakup BAKIŞ

ÖZ

Organik güneş pilleri konusunda araştırmalar son 15 yıl içerisinde büyük bir ivme kazanmıştır. Polimer bilimindeki kat edilen ilerlemeler beraberinde organik güneş pilleri konusundaki araştırmaların sayısında büyük artış sağlamıştır. Organik güneş pilleri üretim süreçlerinde kolaylık ve çeşitlilik, tasarım maliyetlerinin düşüklüğü, değişik yapıdaki yüzeylere uygulanabilirlik kolaylığı gibi özellikleri dikkate değerdir. Organik güneş pillerinde geniş bir polimer yelpazesi bulunmaktadır ve kullanılacak polimer malzemelerin yapısında çok karmaşık olmayan kimyasal proseslerle değişimler sağlanarak istenilen fotoelektriksel, fiziksel veya kimyasal özellikleri elde edebilmek mümkündür. Bu tezde çeşitli bulk heterojunction organik güneş pilleri konusunda çalışılmıştır. Öncelikle standart bir verimde bir ITO-PEDOT:PSS-P3HT/PCBM-Al güneş pili üretimi yapıldı başarılı bir şekilde üretildi. Numune hazırlama prosedürleri, kaplama yöntem ve ortam şartları , katman kalınlıklar, optimize edildi Güneş Hücresi katmanlarının yapısal özellikleri AFM, Sem ,ve Fotolüminesan spektroskopi yöntemleri ile incelendi. İkinci olarak optimize güneş pilinin yapısına Altın Nano Parçacıklar anot ve katot katmanları arasına belirli oranlarda katkılanması ile pilin yapısındaki güneş ışığı çevirim verimleri incelenmiştir. Son olarak da üretilen bütün pillerin kısa devre, akım yoğunluğu , açık devre voltajı , dolum faktörü , enerji dönüşüm faktörleri ölçülmüştür.

Anahtar Kelimeler: Organik güneş hüceleri, ITO, İletken polimerker, Bulk Heterojunction

To my dear Family

ACKNOWLEDGEMENT

TABLE OF CONTENTS

LIST OF TABLES

TABLE

LIST OF FIGURES

FIGURES

LIST OF SYMBOLS AND ABBREVIATIONS

SYMBOLS /ABBREVIATIONS

A	Area
α	Polarizability of the particle
AFM	Atomic Force microscopy
AM-1.5 G	Air Mass 1.5 Global
BHJ	Bulk hetero junction
c	The speed of light
C_{abs}	Absorption cross-sections
C_{scat}	Scattering cross-sections
CuInSe2	Copper indium Selenium
DC	Direct current
e.m.f	Electro motive force
e.V.	Electron volt
E	Energy
Ep	Plazmon energy
ε_p	Dielectric function of the particle
FF	Fill Factor
GaAs	Gallium arsenide
$\hbar$	Planck constant
IEA	International Energy Agency
I_{SC}	Short Circuit Current
J	Current Density
K	Boltzmann's constant
LSPR	Localized surface plasmon resonance
MPP	Maximum power point
η	Efficiency
NREL	National Renewable Energy Laboratory

OFET	Organic field effect transistor
OSC	Organic solar cell
π	Pi
P3HT	Poly(3-hexylthiophene-2,5-diyl)
PCE	Photo conversion efficiency
PEDOT:PSS	Poly(3,4-ethylenedioxythiophene) Polystyrene sulfonate
Pin	Incident Power
Pmax	Maximum Point
Pout	Output Power
PT	Polythiophene
PV	Photovoltaics
R_S	Series Resistance
R_{SH}	Shunt Resistance
q	Electronic charge
QE	Quantum efficiency
R2R	Roll-to-Roll
RF	Radio Frequency
σ	Sigma
SC	Solar Cell
SFM	Scanning force microscopy
SPM	Scanning probe microscopy
τ	Relaxation Time
THF	Tetrahydrofuran
Voc	Open-Circuit Voltage
ω	Frequency
ω_p	Bulk plasmon frequency

CHAPTER 1

INTRODUCTION

1.1 MOTIVATION

Energy is the one most indispensable consuming item of the human being throughout its life duration. In our daily life we cannot sustain our routines without energy and it is an essential part of our daily lives. We use energy to produce our essential requirement by energy conversions. Humanity had been in a spirit instead of reaching the power via the energy which is a major driver of economic wealth, and still today this act strongly pursue, all researches based on obtaining energy.

Fossil energy sources take an important part in the global energy consuming volume. World energy market value in world about 1.6 trillion dollars and it is mostly provide by fossil energy sources [1]. In organization of petroleum exporting countries, it will become highly more concentrated to maintain of petroleum industry's intended growth of until 2030. [2]. The easiest way for production of energy, fossil fuels, has been most preferred source. Easy usage, simple to find and cheapness was some of the advantages. Nevertheless even the world started to globalization, those advantages could not sustain these more serious disadvantages such that global warming, depleting of fuel sources, irreversible environmental pollution and significant harmful effects on planet. Consequently , increasing ratio of carbon dioxide in our atmosphere considerably influence the greenhouse effect which causes increase on the global temperature [3].The results of these kinds of chances are already seen by an incensement in the intensity and frequency of natural disasters [4]. Even the world energy demand continues increasing, and the cost for natural carbon resources are rising, new alternatives for the low cost production of energy from renewable resources are need to investigated [5,6].

CHAPTER 2

SOLAR CELLS

2.1 INTRODUCTION

The principle of solar cells is operated by converting sun photons energies into electricity by using semiconductor materials electronic properties. Photovoltaic effect is basic mechanism for solar cells [7]. The solar cells (SCs) cells have widely started investigated since the 1950's when the first silicon based solar cell. The achieved efficiency which was about %6 , and developed at Bell laboratories [8]. It was the basic physical process, by which the semiconductor material converts electromagnetic radiation (sun light) into electric power. Bell found the photovoltaic effect while experimenting with an electrolytic which is made up with two metal electrodes [9]. In 1839 another investigation was done, by E. Becquerel. He investigated that two type brass plates immersed in a liquid produced a continuous current during illumination of photons. After 1870s, W. Smith, and friends discovered a photo voltaic effect in selenium (Se) element. Then, C. E. Fritts setup an amorphous Se sheet on a metal support and covered the Se with thin and transparent gold film. It is reported that Se array produced an electrical current which was constant, continuous and adjustable force with intensity of sunlight. On that day, quantum theory was not explained and there was no adequate mechanism for explanation about his experiment of converting sunlight into electricity current. Then a sample photo voltaic sent to Werner Siemens in Germany who was one of the most respected scientists in electricity studies at the time. Fritts's theory is also verified by Siemens's investigations. Nevertheless, the power conversion efficiencies (PCE) of the thin film of amorphous selenium and cuprous oxide solar cells were under 1%. [10].

This dilemma finally was solved after development of the based silicon solar cell in 1941 by Russell Ohl. About twelve years later, followed by the commercialization of silicon technology needed to fabricate the transistor for electronics, G. Pearson, and his team, demonstrated a silicon based solar cell which had a 6 percent PCE when used in sunlight. Later in the 1980s silicon based solar cells, as similar as cells made of gallium arsenide, which achieved efficiencies more than 20 % had been fabricated. In 1989 a concentrator solar cell fabricated which collects concentrated sunlight onto the cell surface and 37 % efficiency achieved through the enhanced intensity of the incident photon. Higher efficiencies are possible by link of cells within different semiconductors electrically and optically in series but at the same time increased fabrication cost and a complexity are other results. Now various solar cells are available widely and commercially with different efficiencies and costs [11].

The expenses of solar cell are always given by the watt peak. Prices of solar cells are varies proportional with the size of panel. Nearly 50 %-60 % of cost is consumed for installation process and rest of are for material manufacturing. Also all these suppositions are related with the location where the solar cells are installed. From 2004 to 2013, the installed solar cells total capacity potential has increased from 3,7 Giga watts (GW) to 139 to GW (shown in Figure 2.1).
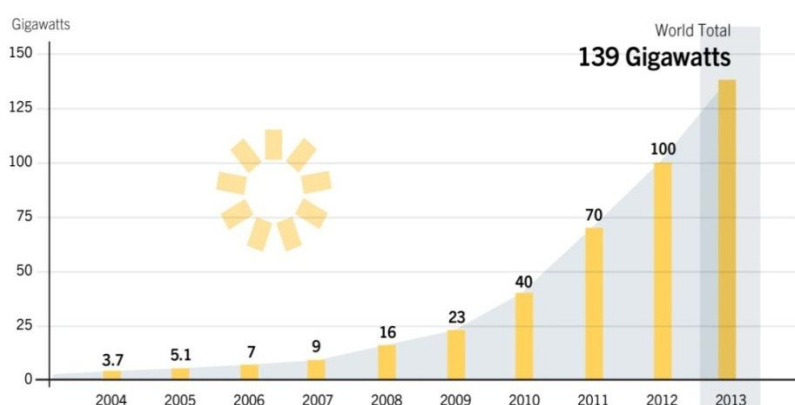
Figure 2.1. Global solar cell installation amount from 2004 to 2013 [12].

2.2 SOLAR CELL GENERATONS

Solar cell technologies are conventionally divided into three types of generations. First generation solar cells: solar cells are large scale, single junction devices. Majority of the production is based on silicon wafers which include single crystal and multi-crystalline silicon and typically demonstrate about 15-20 % energy conversion performance. Solar cell markets' %90 is dominated by these types of solar cells. Their long term stability is more attractive than their performances. However, they are not adequate and adapted for a large scale of usage area and from fabrication to installation they require more energy. Single crystal solar cells and multi crystal solar cells are known types of first generation solar cells [12].

The second generation solar cells include amorphous silicon, CIGS and CdTe, and their energy conversion performances are about 10 - 15 %. Si wafers is the main expense of production. The second generation solar cells provide lower usage of silicon wafers and material consumption with parallel this is decreasing production costs arises when compared to the first generations. Still second generation solar cells can also be produced and possible to find commercially. At the same time production of second generation solar cells includes high energy consuming processes such as vacuum processes and high temperature treatments which increases the production costs. The second generation solar cells are based limited elements and this is a increasing factor in the price.

Third generation solar cells based on improving the solar cells which are present and use in industry. Third generation SC offers novel approaches to photovoltaics (PV). As aim, high efficient devices production by developing and using thin-film, and second generation deposition methods can be counted. [13].

Today's popular novel generation solar cells are being produced from a wide range of materials such that nanowires, nanotubes, polymer inks, silicon wires, using classical printing press techniques, organic and conducting dye. At the present time most of the studies and investigations on third generation solar cells is being done in scale of laboratory and being highly developed by commercial companies. [14].

Nonetheless third generation includes experimentally expensive but high efficient solar cell types. Multi junction solar cells are belongs to this type and provides the highest solar cell performance record of photo voltaic field. Only this type has some extended commercial applications because of their high cost of production. Organic solar cells (OSCs) or plastic solar cells are polymers and they provide various incomings such that easy, fast fabrication and inexpensive large-scale production that use of materials which are easily exists with potentially lower expenses. Polymers or plastic based solar cells can be produced with common applying industrial technique: roll-to-roll (R2R) methods which can be likened to the offset printing methods. Even though the performance and environmental degradation of the third generation solar cells is still limited when compared with first and second solar cells generations, they have a grand investigation and study potential. [12, 15] Cost efficiency analysis for each of generation is shown in Figure 2.2.

Theoretically , solar cells can convert incident photons energy to electricity at an efficiency near to the Carnot 95% limit for the sun modeled as a black-body at T_1=5726 °C (the sun surfaces' the temperature), and a solar cell which can operate at room temperature (T_2=25°C)

$$\eta = 1 - (T2/T1) = 1 - (300/6000) = 0,95 \tag{2.1}$$

$$A = \pi r^2 \tag{2.2}$$

Actually, 93.3% yield is the maximum theoretical and slightly different from 95%. It shows that more improvements are potentially achieved, with incensements from the theoretical 31% energy conversion efficiency limit which had calculated for a single junction solar cell in 1961 (see Figure 2.2) [16].

Thermodynamic efficiency limit defined as the absolute maximum theoretically energy conversion efficiency of sunlight energy to electricity. Carnot limit gives value of about 86%, due to the temperature loss of the photons emitted by the surface of sun.

"Third generation" technologies can be divided into 3A and 3B. Cells in 3A aim for very high efficiencies, and thus the allowed cost of the cell can be quite high. Possible and existing technologies include heat carriers, electron-hole pair creation, and

thermo photonics. Active devices have yet to be produced .The goal of 3B devices is to achieve moderate efficiency with very lower costs.
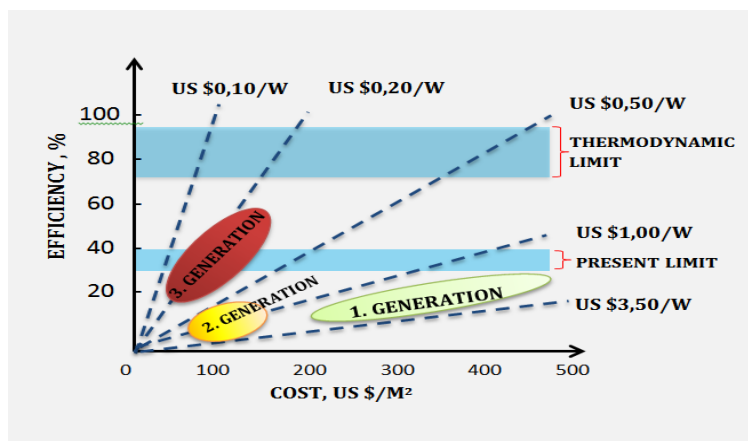
Figure 2.2 Solar cell costs and efficiency [16].

Cost efficiency analyses for each of the generations are shown in Figure 2.2 [16]. Also Total achieved efficiencies of solar cell development are shown in Figure 2.3.
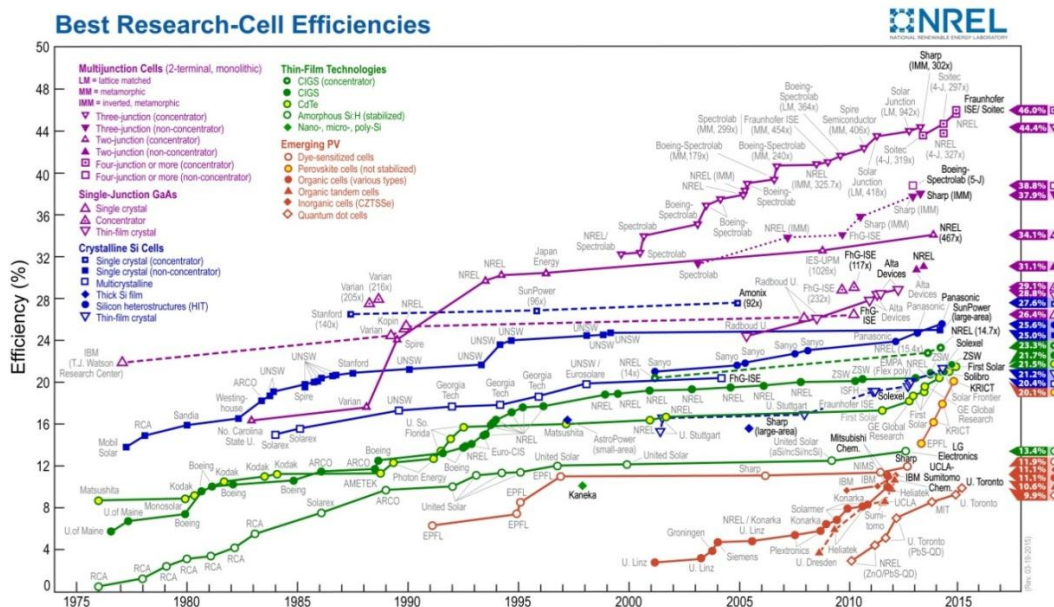
Figure 2.3 Solar cell efficiencies [17].

2.3 WORKING PRINCIPLE OF SOLAR CELLS

A solar cell converts sunlight directly to electricity. Working principle depends on some ideas of quantum theory. Photons are the energy packed that formed by light whose energy varies by the color or frequency [15]. Visible photon's energy is adequate to excite electrons which stated into structure of solids, until levels of higher energy where they are freer to mobile. A remarkable instance of this is the photoelectric effect, was explained and resulted by Einstein in 1905, (shown in Figure 2.4) where blue or ultraviolet incident light supplies necessary energy of electrons for moving completely from the metal surface.
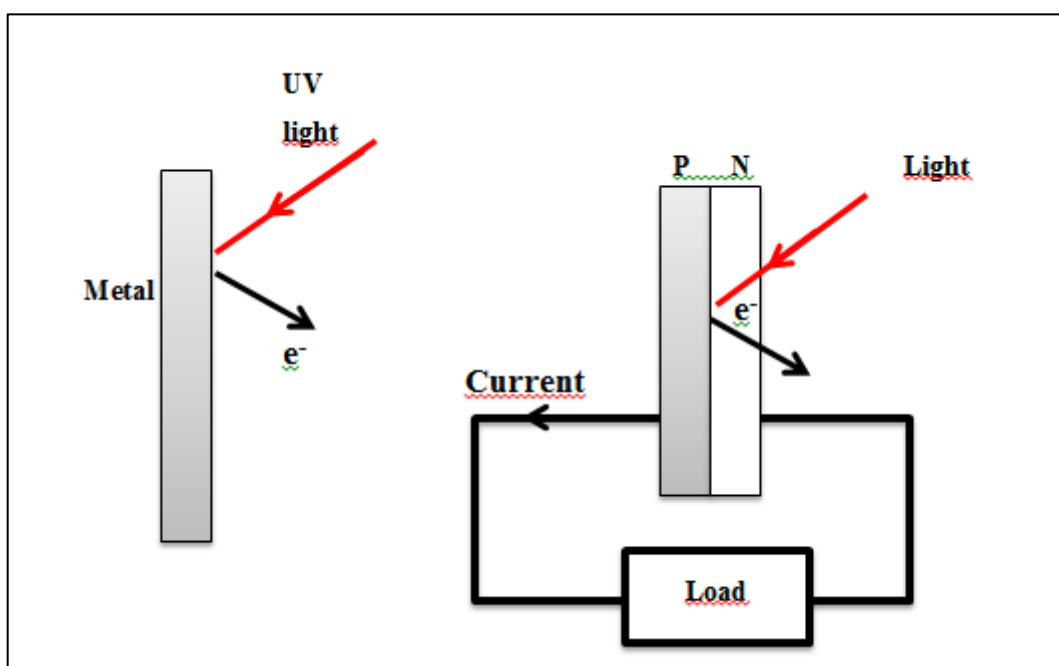
Figure 2.4 Comparison of the photoelectric effect [15].

Generally, when photons are absorbed by object, photons aren't remained to excite electrons from lower states of energy to higher energy states of the illuminated material. Also the excited electrons have a fast turn back tendency to their ground state. Also, there is some built in asymmetry (internal electric field) in a photovoltaic device, which moves the excited electrons away before they can relax, and supply electrons to an external circuit. A potential difference is generated by the extra energy of the excited

electrons, or electro motive force (e.m.f). E.m.f moves the electrons through a load in the external circuit for doing electrical work [17]. Figure 2.4 demonstrates of photo electric effect of material at left side, where ultra violet light releases electrons from the metal surface with the photovoltaic effect in a solar cell (SC) (right side). The photovoltaic material requires having several spatial asymmetries. For example contacts which includes various type of electronic properties, leads for driving the excited electrons from one side to another of the external circuit.

A bound state of an electron named as an exiton which is a pair of electron and hole and combined to each other owing to the electrostatic Coulomb force. Exiton is an electrically neutral quasiparticle that consists in insulators and semiconductors (Figure 2.5). The exciton is estimated as an basic excitation of condensed matter that can transport energy without changing net electric charge [18].
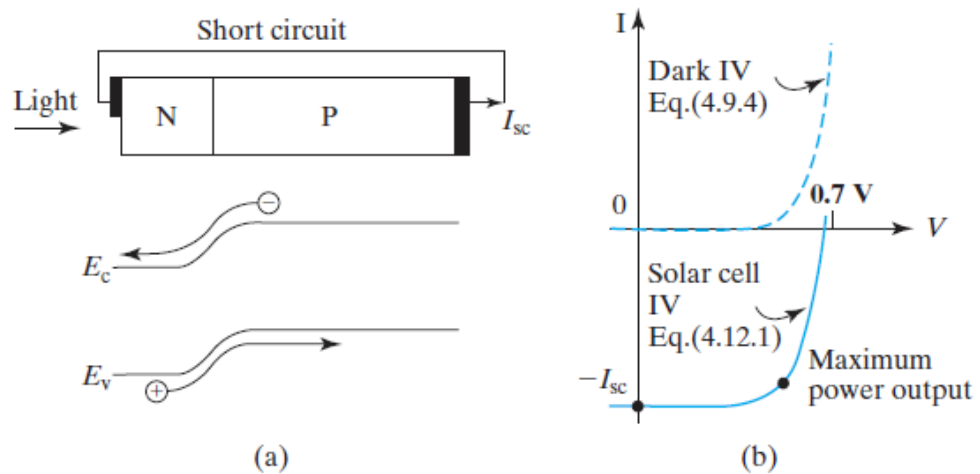
Figure 2.5 (a) Production of current by photovoltaic effect in P-N junction at V = 0. (b) Solar cell I-V product is at 4. quadrant (negative), due to specify power generation [23].

The contribution to the photocurrent is defined as;

$$J = J_n + J_p = \mu_n n \nabla E_{F_n} + \mu_p p \nabla E_{F_p} \tag{2.3}$$

Where;

J: Current Density A/cm^2

J_n :   Spatial density of conduction band electrons A/cm^2

J_p: Spatial density of holes in a material A/cm^2

μ_n :   Mobility of electrons cm^2/Vs

μ_p :   Mobility of holes cm^2/Vs

E :   Electric field intensity which applied in V/cm

Fermi Level energies E_{Fn} and E_{Fp} values equal to each other and these values are constant when the semiconductor material is in equilibrium. At the same time photocurrent equals to zero (J =0). For operating the photovoltaic mechanism, the incident light should produce a gradient in minimum one of the Fermi levels (E_{Fn},E_{Fp}). The electric field is different from zero under the incident light and a net drift caused by this reason. Despite the electric field is equal to zero, carrier densities include a gradient. A net diffusion current may be caused by this gradient. At the equilibrium conditions an electric field occurs. This electric field is also called as "built in field".

Charge separation in a semiconductor can be possible with gradient in the vacuum level, work function, the electron affinity, band gap and band densities of states.

2.3.1 Vacuum Level

Vacuum level states to the energy of a free immobile electron that is outer side of any material.

2.3.2 Densities of States

Energy distribution between identical particles depends partly onto number of available states in a given energy gap. This density of states gives the number of states per unit volume as a function of energy in an energy interval. In particular for situations where the available states are separated, the term "statistical weight" is from time to time used synonymously,

2.3.3 Band Gap of Material

In field of solid state physics, band gap, is a type of energy interval in solids where the existence of electron states cannot possible. In Solids materials electronic band structure graphs' the band gap express the energy difference between the top of the valence band and the bottom of the conduction band (in electron volts) in semiconductors and insulators materials.

2.3.4 Work Function Of Material

The work function is the minimum energy requires for moving an electron from the Fermi energy level, (E_F) to vacuum energy (E_{vac}) it is defined by;

$$\Phi_{\omega} = E_{vac} - E_F \tag{2.4}$$

It is possible to obtain various work functions by using different materials and also by doping variations. Work function is lower for n-type than p type semiconductor, $\Phi_n < \Phi_p$, because At the band gap of a semiconductor material, Fermi levels depends upon doping properties. Junctions that have different work functions produce an electrostatic field.

In solar cell field, the mostly used method for determining the charge separating field is by differentiating amounts of the doping ratio in semiconductor.   Each of the steps is crucial for the efficient power generation and there are many loss mechanisms involved in this sequence. The terms donor and acceptor refer to materials with either high ionization potential (donor) or high electron affinity (acceptor). The free charge collection at opposite electrodes is assured by the asymmetric ionization energy or work function of the electrodes [19].

2.4 BASIC SOLAR CELL PARAMETERS

A Solar cell (SC) can behave as a energy container or a accumulator in a basic electric circuit (shown in Figure 2.6). Even light excites SC, it starts to produce a voltage or electro motive force.

The voltage incensement occurs while the terminals are isolated this is named as the open circuit voltage (V_{OC}). when the voltage across the solar cell is zero a current though the solar cell is called as short circuit current (I_{SC}).

solar cell

battery

(a)

(b)
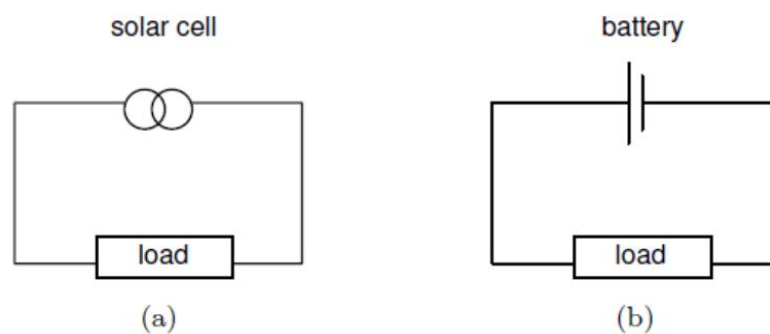
Figure 2.6 A solar cell may be used as a battery in a circuit.

2.4.1 Equivalent Circuit Of A Solar Cell

The equivalent circuit is used as a model which is help to describe the electric behavior of similar or equivalent based devices with basic ideal electrical equipment such as current sources, voltage sources capacitors, resistors, and diodes.
It is possible to model an ideal solar cell a current source in parallel with a diode; a parallel shunt resistance and a series resistance components can linked to the circuit (see Figure 2.7).
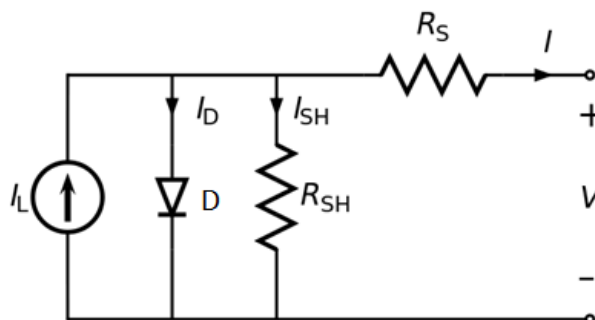
Figure 2.7 The equivalent circuit model of an ideal solar cell [20].

2.4.1.1 Shunt Resistance

When the charge carriers recombine closest to the disassociation site Shunt resistance occurs. In electric circuits diodes cannot conduct current and it should be an adjustment and voltage determined by R_{Sh} +R. For an ideal solar cell, Shunt resistance should be high [7,20].

I_L: A current generated by light I_L. This current is generated by dissociation of excitons as electrons and holes after photon energy absorption. I_L does not allow any recombination but just depends on the charge carrier formation efficiency

R_{Sh} : is shunt resistor. it takes an significant role in the performance of a solar cell. In circuit a leakage current resistance leads to absorb more current, For efficient solar cell , this resistance should be infinite

R_S: The series resistor occurs in a circuit due to the electron and hole mobility in a solar cell. Mainly can be occur at contact layers of solar cell . defects and barriers in system may effect mobility of charge carriers. Increase of distance that the charges have to move to the collecting electrodes also increases Rs. a ideal solar cell it is expected that Rs should be zero.

D: is diode: It expresses the conductivity which is asymmetric in the solar cell. In OSCs, this is because of the PN junction formation have a blockage behavior in only one way current direction.. In a ideal solar cell it is expected that R_S should be zero and R_{Sh} should be infinite. But in terms of real in OSC s R_S is different from zero and R_{Sh} is more than 1000 ohms. These values will widely different in OSC due to mobility and charge recombination. From the equivalent circuit;

$$I = I_L - I_D - I_{SH} \tag{2.6}$$

Where

I :   Output current (ampere)

I_L Photo generated current (ampere)

I_D: Current of diode (ampere)

I_{SH}:   Shunt current (ampere)

The current through these elements is directed by the voltage across them:

$$V_j = V +(I .R_s)$$
(2.7)

Where;

V_i :   The voltage across both diode and resistor R_{SH} (volt)

V :   The voltage across the output terminals (volt)

I :   The output current (ampere)

R_s: The series resistance (Ω).

In solar cell P or N type semiconductor allows mainly free charge carriers (electrons or holes) for passing through. Therefore, for driving a current through the diode under condition of no illumination (dark), the electrons need to establish a recombination at someplace in the diode, the rate of recombining is limited by the density of minority carrier. This charge carrier density is proportional to the Boltzmann factor $e^{-E/kT}$, where E is the barrier across the P-N junction. With the amount of the applied bias, the barrier decreases because of P-N role. So that, the density of minority carriers show an incensement exponentially with applied bias, and so does the recombination rate and the current through the diode. Therefore it can be calculated mathematically:

$$J=Ae^{BV}+C$$
(2.8)

For V = 0 and J = 0.   A and C can be calculated. Negative V, J saturates to the so-called saturation current J_0. This current, occurs between 0.1 and $1pA/cm^2$. If, it is taken V towards minus infinite, and it can be calculated a value for C. The assignment of B to a physical entity is done with the Boltzmann factor, where E is replaced by the voltage B:

$$B = qV/kT,$$
(2.9)

Where

$$k = 8.61758 \times 105 \text{ eV/K}. \tag{2.10}$$

Then, kT/q and the thermal voltage (V_{th}) defined as;

$$V_{th} = 25.8 \text{ mV at 300K}. \tag{2.11}$$

By the Shockley diode equation, the current diverted through the diode is:

$$I_D = I_0 \left[exp \left(\frac{qV_j}{nkT} \right) - 1 \right] \tag{2.12}$$

I_0 The reverse saturation current (ampere)

q   Elementary charge

n   Diodes ideality factor ("1" for an ideal diode)

T   Absolute temperature

K   Boltzmann's constant

$$kT/q \approx 0.0257 \text{ volt At 25°C} \tag{2.13}$$

By Ohm's law, the current calculated through the shunt resistor is:

$$I_{SH} = \frac{V_J}{R_{SH}} \tag{2.14}$$

Where R_{SH} : Substituting these into the first equation produces the characteristic equation of a solar cell, which relates solar cell parameters to the output current and voltage:

$$I = I_L - I_0 \left[exp \left(\frac{q(V+IR_S)}{nkT} \right) - 1 \right] - \frac{V+IR_S}{R_{SH}} \tag{2.15}$$

A different substitute derivation produces similar equation,. Both alternatives are yield exactly the same results.

Application for extracting the characteristic behavior of equation is possible with nonlinear regression. The values that obtained are represents solar cell behavior. It is not

possible to calculate the reverse saturation current, ideality factor, series resistance, and shunt resistances with direct methods.
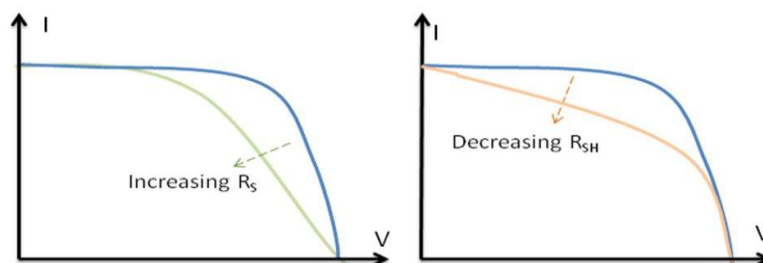
Figure 2.8 Differentiation of R_S and R_{SH}.

Theoretically when an operating voltage applied, the current can be determined for specific voltage. In an ideal cell, R_{SH} assumed infinite and provide an alternate route for current to flow, At the same time R_S be expected zero, with resulting in no later voltage decreases before the load. When the R_{SH} decreases and Rs increases, fill factor starts to decrease and due to this maximum power diminishes. as shown in Figure 2.8. If R_{SH} is decreases in a big amount, V_{OC} will decrease, same as when R_S increases I_{SC} decreases.
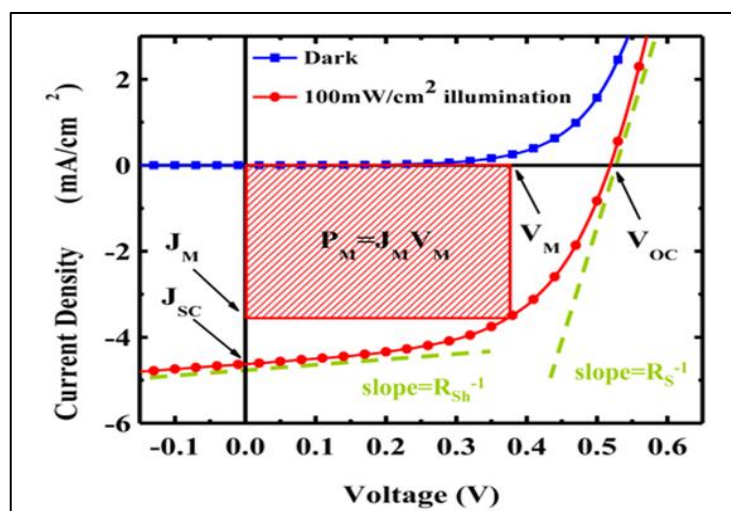
Figure 2.9 R_{SH} and Rs resistances on solar cell I-V characteristic diagram.

It is feasible to acquire, R_S and R_{SH}, from the slopes of the I-V curve at V_{OC} and I_{SC}, respectively. At V_{oc}, resistance proportional to the series resistance but it is more than the R_S. R_{SH} is defined from the slope of I_{SC}. point respectively, R_S and R_{SH} at I_{SC} and at V_{OC} can be defined, as shown in Figure 2.9

2.5 VOLTAGE CURRENT RELATIONS

2.5.1 The Open-Circuit Voltage

During operation of the solar cell at zero current, a voltage passes the output terminals and this voltage is called as open-circuit voltage. There should be assumptions such that the shunt resistance is high and adequate to dismiss the final term of the characteristic equation.

The open-circuit voltage V_{OC} is:

$$V_{OC} \approx \frac{nKT}{q} ln \left(\frac{I_L}{I_0} + 1 \right)$$
(2.16)

2.5.2 Short-Circuit Current.

During operation of the solar cell at short circuit, voltage is zero and the current *I* passes to the output terminals is called as *short-circuit current*. For an high efficient solar can Isc is:

$$I_{sc} \approx I_L$$
(2.17)

It is not possible to take out any power from the solar cell while operating at either open circuit or short circuit conditions

2.5.3 Fill Factor (FF)

The squareness amount of I-V curve defines the Fill factor. This value depends on the ratio of two areas shown in Figure 2.10. This ratio will be unity under ideal conditions i.e. when there are no parasitic resistance losses in the devices. Resistance

has a great impact on PV devices. Shunt resistance and series resistance are important. Fill factor. (FF) is defined as;

$$FF = \frac{P_{max}}{I_{SC} \cdot V_{OC}} = \frac{I_{MP} \cdot V_{MP}}{I_{SC} \cdot V_{OC}} \qquad (2.18)$$
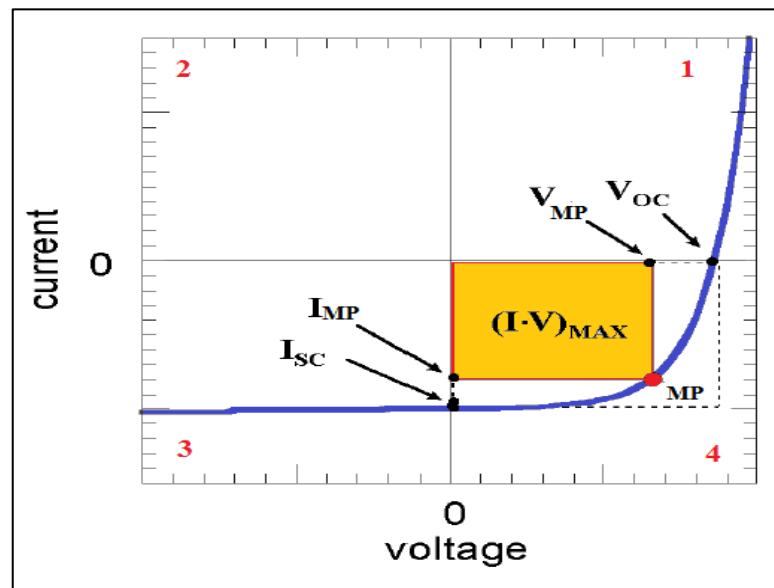
Figure 2.10 I-V diagram of a solar cell [20].

2.5.4 Maximum Power

Maximum Power defines at : $P_{MP} = I_{MP}$ x V_{MP} Maximum power value I and V diagram. It can be calculated for each I and V points (P=I x V). Maximum power point can be determined by defining the maximum value between I_{SC} and V_{OC} points.

2.6 POWER CONVERSION EFFICIENCY

This is the ratio of electric power that generated from solar cell to the incident light energy power. The maximum power production of solar cell should be defined for calculating power conversion efficiency.

It can be calculated as in equation 2.5

$$\eta AM\ 1.5 = Pout\ /\ Pin \tag{2.19}$$

$$\eta AM\ 1.5 = (Jsc \times Voc \times FF)\ /\ Pin \tag{2.20}$$

Where P_{out} = electrical power generated by the cell at maximum power point (mpp), and P_{in} = power of photon. [7, 8, 20, 21].
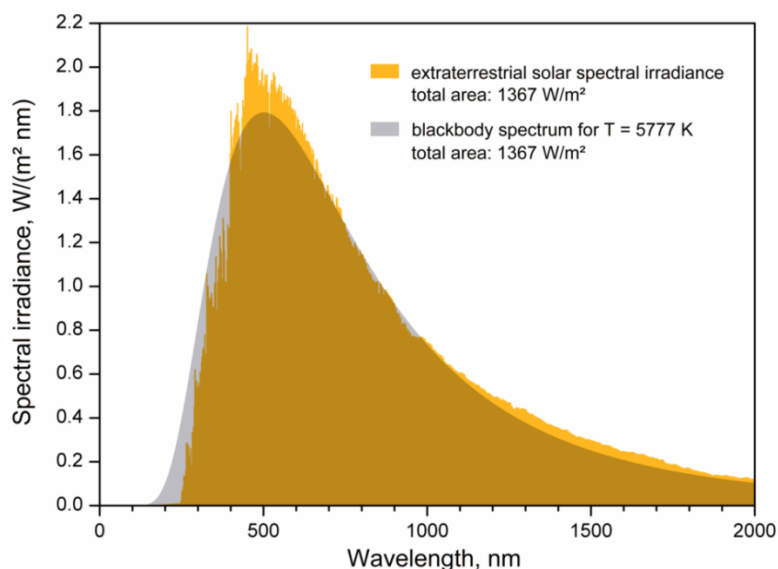
Figure 2.11 Solar spectrum:Air Mass 1.5 [23].

Solar cells cannot absorb photons and generate electric in the same efficiency at all wave lengths. Because, the power conversion efficiency is connected with the light source power and   spectrum of illumination source. At the surface of earth sun light may sat with different factors such as angle, location etc. For comparing efficiency of photo voltaic equipment, the Air mass spectrum AM1.5 G spectrum in Figure 2.11 is the most known spectrum standard . In laboratory conditions, it is not easy to mimic or create Sun spectrum with devices. For standardization of common illumination sources (lamb etc.) , the external quantum efficiency can be used as correcting models [22].

2.6.1   Photocurrent And Quantum Efficiency

Solar cell generates photo current with incident light at short circuit condition. This current is dependent to the incident light

For establishing a relation with incident light spectrum and photocurrent density (Jsc) , The quantum efficiency (QE) of solar cell should be known. The probability of a photons' an electron deliver   It can be calculated as in equation 2.17

. $$J_{SC} = q \int b_s(E)\, QE(E) dE \tag{2.21}$$

Where;

QE(E)   the probability which Energy of incident photon (E) will transfer one electron to the circuit.

b_S(E)   Flux density of incident spectral photon

E   Photon energy amount in the range

E+dE   Incident photon on unit area in unit time and

q   Charge of electron.

QE of material is not dependent to the incident photon but it is related with materials efficiency absorption, charge separation and charge collection.

QE is a quantity for describe solar cell performance under various conditions. of photons shown in Figure 2.13 . QE and spectrum can be expressed as functions of photon energy or wavelength, λ. The correlation between energy E and wavelength λ is defined by:

$$E = \frac{hc}{\lambda} \tag{2.22}$$

Where

h   Planck constant and

c   The speed of light in vacuum.

An appropriate rule for converting between photon energies, in electron-volts, and wavelengths, in nm, is E/eV.
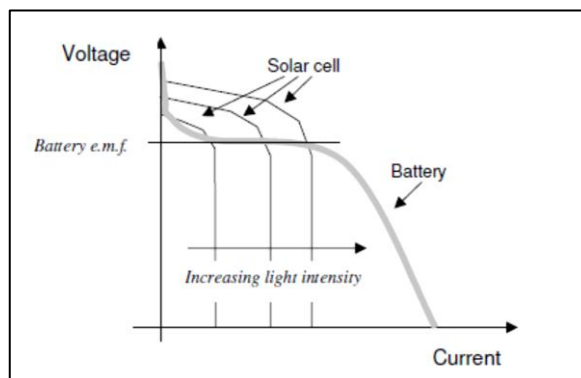
Figure 2.12 Voltage-current curves of a battery (grey) and a solar cell under different various illumination conditions.

In Figure 2.13 By integration of photon energy over quantum efficiency and photon flux density's' product, the short circuit photocurrent can be obtained. Having the high quantum efficiency at wavelengths where the high solar flux density is a desired condition.
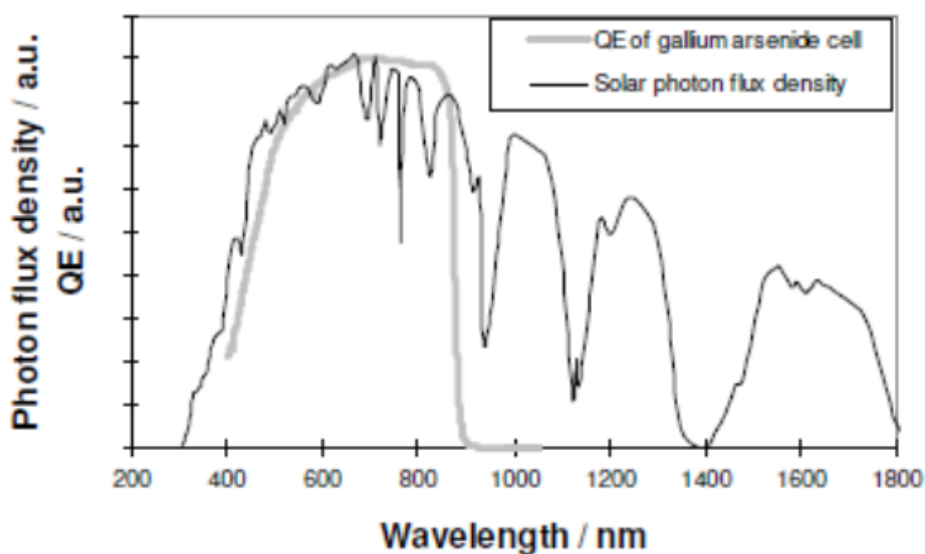
Figure 2.13 Quantum efficiency of GaAs solar cell compared to the solar spectrum.

The PV cell supplies a constant current for a particular illumination level; meanwhile the voltage is mostly determined by the load resistance. In solar cell, it is common plotting the data in the opposite way with current and voltage values represented on the vertical and horizontal axis respectively. This is because solar cell is basically a current source meanwhile a convention al battery behaves as voltage source.

CHAPTER 3

ORGANIC SOLAR CELLS

3.1 INTRODUCTION

Silica based inorganic solar cells are major production component of the Photo Voltaic industry. High installation costs and complicated fabrication processes of inorganic solar cells are their disadvantages. Solar cells have a part less than 0.1% of the total energy conversion in the world International Energy Agency (IEA) [24].

Organic solar cells (OSC) made of polymers which provide fast, simple, low cost and large volume processing, since polymers have the opportunity to be solution processed, which literally means printing solar cells on roll-to-roll (R2R) machinery like newspapers. Typical OSC devices have a layered structure and are commonly considered organic if the active absorbing layer involves only organic compounds, meanwhile the other layers (electrodes, etc.) can be consisted by inorganic materials such that metals. Often the OSC field includes a category of hybrid solar cells, in which the active layer contains some inorganic quantum dots doped into the polymer matrix or inorganic metal oxides combined with polymers. There have been a number of reviews discussing the development of OSCs nicely presenting the key events throughout the short history of the OSC field. Although polymer solar cells are developing really fast, there are three main issues that are still remaining unsolved: the improvement of device photo conversion efficiency (PCE), extension of device lifetimes and large scale production. There are a numerous loss mechanisms which result in low PCEs and currently most of the groups in the field are struggling to overcome these mechanisms to improve the efficiency. More and more groups are addressing the stability issue and various approaches are reported for improvement of the device lifetimes. Yet, the improvements are minor and further studies are needed.

Moreover, the experiments show that when a good polymer is developed and the small model devices based on such polymer deliver high efficiencies, it is still a big practical challenge to transfer the device structure to R2R process for large scale production. [19]. In a conventional in OSC structure, weakly coulomb bound pairs of charge carrier (an electron and a hole) are generated by the absorbed sunlight, Determination of opposite charges is too weak even the dielectric constant is too low.
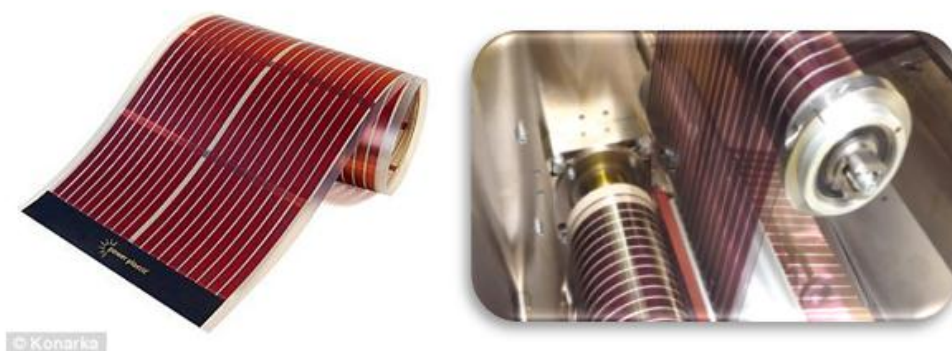
Figure 3.1 Roll-to-roll proccesses (From Konarka).

One of the other characteristic of organic polymeric material is the optical electric properties. These properties can be change by remodeling or alternative molecule structure of monomers. So it is possible to adjust the optical properties for obtaining desired performance of device. This causes to a stronger interactivity of the photo generated negative and positive charges. For this reason, the main optical excitation in organic materials is a single exciton, which is related with nano chemistry techniques. Furthermore , very thin (100 nm) organic films can absorb all the incident light on their surfaces (within their absorption range), which should be compared to an absorption length around 300 mm thickness standard crystalline silica based solar cells, and 1 mm for polycrystalline CuInSe2 thin films [15].Organic polymers generally can be solved in common organic solvents. This situation makes easy to produce OSC s. Thin film production is an essential part of OSC's. To obtain pure, uniform and efficient coatings, Spin coating, [25] Doctor Blading [26] and screen printing [27] methods can be demonstrated. Since start of flexible organic plastics production, OSC s can produce in

amount of roll-to-roll (see Figure 3.1). This is allows cheap, easy, and flexible production process.

3.2 WORKING MECHANISM OF ORGANIC SOLAR CELLS

The mechanism by which the light is converted to electric power in OSCs consists of 4 basic steps (shown in Figure 3.2):
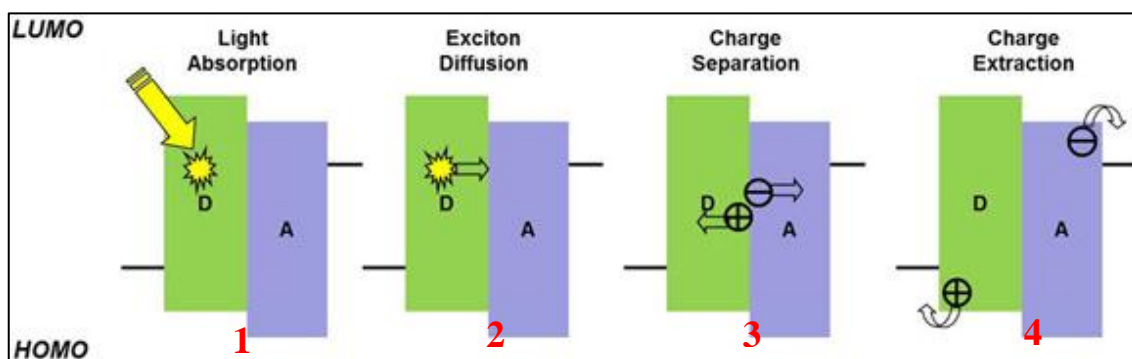
Figure 3.2 Photoelectric conversion mechanism 1-)Light absorption for creating an exciton; 2-) Exciton diffuse on to donor / acceptor interface; 3-) Dissociation of exiton and separation of charge separation; 4-) Transport of charge and collection at the opposite electrodes. (From Sigma Aldrich).

1) The active material absorbs photon by promoting the electron to LUMO while leaving positive charge carrier (hole) in to the HOMO. The pair which is exited is localized by coulomb affinity forces by formation an exciton.

2) The exciton diffusion occurs between donor and acceptor interface.

3) The exciton is dissociation occurs, free carriers forms at the interface of acceptor and donor.

4) Free charge carriers start to transport to the opposite electrodes

The Solar cell (SC) mechanism is operated by the driving force that dissociates the charges.

Optical band gap is another important factor of the light absorbing materials. Optical band gap is defined by difference of HOMO and   LUMO of material. If solar emission spectrum doesn't pairs with the absorption spectrum of the polymer, this circumstance creates main efficiency loses on solar cell. For instance, the band gap of mostly used polymer poly(3-hexylthiophene) P3HT is approximately equal to 1.9 eV. With this band gap it is only able to harvest %22 of incident solar photons [19].

3.3 MATERIALS AND DEVICE STRUCTURE

Material selection is a substantial parameter in OSC s which directly effects efficiency, cost and simplicity of production. For example there are different polymers which have same cost and different efficiencies in market. Appropriate polymer selection affects the production costs directly. To compete with the other common inorganic solar cell, it should be use proper materials in OSC s which lead cheaper production costs and fabrication convenience. Contacts of OSC's are another important parameter which will contribute to the efficiency of solar cell. ITO is one of the more common metals which widely use in organic electronics. Transparency, high conductivity and low resistance are major features. As in polymer selections, contact selections should be done by considering materials Electron volt. (eV) of Conductive and photo-converter components' should be closest or more then Sun's eV.

3.3.1 Factors which affects Organic Solar Cell efficiency

Major factors that directly affect OSC efficiency are in below.

Resistivity of Materials which use in OSC: For efficient charge separation and electron mobility, series resistivity should be less and internal resistivity of solar cell should be more.

Layers' Thickness: For preventing from light absorption loses and to provide efficient charge mobility, thickness should be arrange properly. This factor depends on material which is chosen for fabrication

Light absorption emission and transmission of materials: The behavior of materials under light conditions, defines of solar cell characteristics. Solar parameters directly affected by absorption emission and transmission of materials

Defects and impurities: Generally a lead to voltage loses on OSC. To prevent this, fabrication should be done within proper devices and materials.

3.4 ORGANIC POLYMERS

The electronic structure of organic semiconductors consist conjugated π-electrons. Variations at single carbon or carbon-carbon bonds, forms the base of a conjugated organic material. σ-bonds are single bonds and they are related with localized electron. On the other hand the double bonds include a π-bond and a σ-bond.
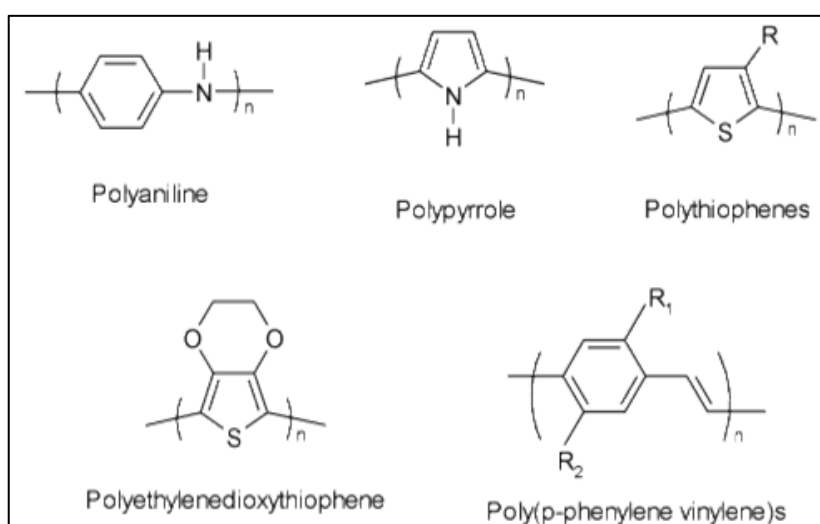
Figure 3.3 Examples of conductive polymers.

The mobility of σ-electrons are lower than π-electrons. π-electrons able to move from one site to another between carbon atoms through the associated coincidence of π-orbitals throughout the conjunction path, which delocalizes the wave functions above the conjugated backbone. The π-bonds can be filled with electrons (Highest Occupied Molecular Orbital - HOMO) or empty (Lowest Unoccupied Molecular Orbital - LUMO). The bands gap of this organic materials change between 1 and 4 eV. In an organic material, π-electron system includes complete electrical properties of material such that light emission and absorption and electronic charge transport and generation. This π-electron system has all the essential electronic features of organic materials: light absorption and emission, charge generation and transport.

A typical OSC consists of a photoactive layer sandwiched between anode and cathode layers. Various material and structure features of polymers can be combined with a wide range of easy and low cost processing methods and this is make polymer based solar cell more attractive against to other solar cells. Organic materials have various advantages such as low cost synthesis and production of thin film devices by simple methods. Polymers which are used in organic electronic field ,are conjugated molecules. Their charge transport and optical absorption properties are dominated partially delocalized π and π P* P orbitals [28].

Polymers are the structures that linked each other with consecutive one or double carbon-carbon bonds and long chained structures which formed by repeating groups. Single bonds are Sigma Bonds. Double bonds forms by one σ- bond (sigma) and one π-bond (pi). Electrons are locates on this conjugated system. Conjugated polymers shown in Figure 3.3 can form as conductive material by making appropriate doping. Polymers can form p-type polymer By oxidizing and form n-type polymer by reducing. At the same time, p-types are material that removed one electron and created positive holes at π-bonds. These holes may fill by π electrons which hop from adjacent molecule [29].

3.4.1 P3HT

Poly(3-hexylthiophene-2,5-diyl) widely known as P3HT. Polythiophenes (PTs) are polymerized thiophenes, a sulfur heterocycle. PTs can show conductive characteristic within addition of electron or removing of an electron from the conjugated π- orbitals by doping method. Investigations about PTs have intensively increased over

last thirty years. PTs optical properties are related with solvents, temperature, and other molecules that connected [30].

P3HT has low molecular weight and regular molecular structure. Due to this, P3HT is an appropriate material for deposition techniques which such that ink jet and slow drying deposition where surface roughness and gelling/aggregation avoid to be expected.P3HT is high degree of solute in chlorinated solvents such as, chlorobenzen and deriatives .Xylene, toluene and Tetrahydrofuran are non-chlorinated solvents which are appropriate for lower molecular weight P3HT materials due to their enhanced solubility [31].

3.4.2 PEDOT:PSS

A member of Polythiophene based conducting polymers, poly(3,4-ethylenedioxythiophene) (PEDOT) in Figure 3.4 has been used widely used in various applications such as OSC s, organic light emitting diode, antistatic and anticorrosion materials ,various conductive surface coatings, electrode materials in batteries, super capacitors, displaying devices, and biosensors and many more.
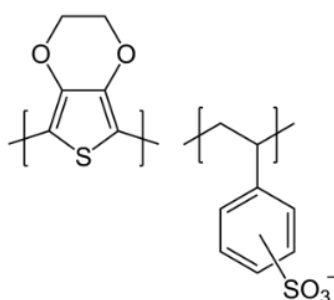

Figure 3.4 PEDOT:PSS.

PEDOT use in solar cells is because of its visible range transparency, high hole conductivity (550 S/cm), chemical and electrochemical stability and thermal stability. PEDOT is made of its monomer EDOT. There are various methods have been reported to prepare PEDOT such as electrochemical oxidation, chemical vapor polymerization,

photo electrochemical polymerization, chemical methods. PEDOT is not soluble in many common solvents and moreover it is not stable in its neutral state. It oxidizes very fast under air /moisture contact [32]

Addition of Polyelectrolyte materials such as polystyrene sulfonate (PSS) provides chemical stability and uncomplicated applicability. The aqueous solution of PEDOT:PSS is highly conductive and PEDOT remains in its oxidized state. The work function of PEDOT is 5.2 eV which makes it as a suitable hole transporting material for OSC s. PEDOT:PSS used as a hole transporting material in organic electronic. The aqueous solution of PEDOT:PSS is more appropriate for the thin, transparent and conductive surface coating on different applications. The structure, electrical conductivity and transparency of the film depends on the particle size, solvent, various amount of doping concentration, and method of preparation. PEDOT can be prepared on different surfaces by various methods such as; slot-die coating, spin coating chemical vapor polymerization, ink-jet printing, spray coating, electrochemical polymerization techniques. Thickness of coating on a substrate can be controlled by concentration of monomer, solvent type, electrode type, coating media etc. [33-34]. Spin-coating is an excellent technique to obtain high-quality multilayer thin films for solar cells, in small scale and for research purposes. It is a quite easy, fast, technique for preparation of uniform, well-integrated nano/micro layers in organic and inorganic devices [35-36]. Xia et al. achieved a significant conductivity improvement by spinning of PEDOT:PSS in co-solvent of water and an organic solvent [37]. Also PEDOT is an polymer which is well known to be a hole injector (collector) and a blocking electron layer.

3.4.3 PCBM

PCBM is a fullerene derivative [6,6]-phenyl-C61-butyric acid methyl ester. PCBM (see Figure 3.5) is a fullerene derivative of the C60 first synthesized in the 1990s by Fred Wudl's group [39]. It is being investigated for OSC s [38]. It is an electron acceptor material and is mostly used in OSC s and organic electronic applications in combination with electron donor materials such as P3HT or other organic polymers.

It is an advantage of using PCBM as an electron acceptor due to more solvable in chlorobenzene then fullerens.
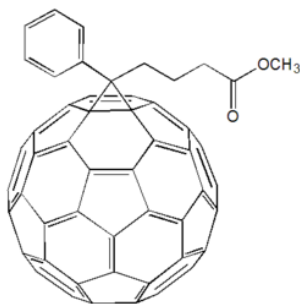
Figure 3.5 PCBM.

This feature provides miscible donor/acceptor blends which a substantial feature for printable OSC s.

3.5 DEVICE STRUCTURE

A conventional OSC consists of a photoactive layer deposited between two different electrode layers which one of electrode should be transparent due to transmitting incident photons on to the photoactive layer, as seen. Figure 3.6.
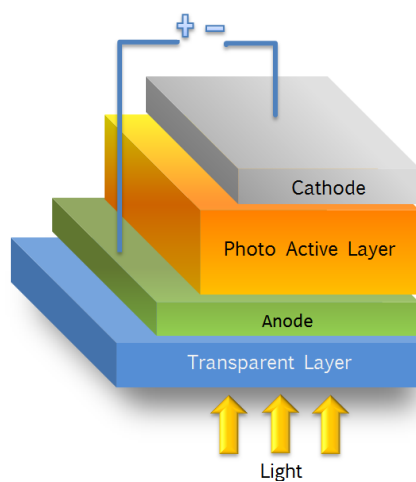
Figure 3.6 Layout of organic solar cell.

When incident light excites photoactive layer, due to the internal electric field, charge carriers are created which ensured by the asymmetrical ionization energies/work functions of the anode and cathode layers. Consisted charges are transported and collected to the external circuit

Device structure of OSC s is very important for efficiency. For an efficient creation and dissociation of excitons, structure should be adjusted finely. For efficient charge separation and transfer, fabrication process should be sensitive. There are various types of structures, such as planar heterojunctions, single layer devices, bilayer heterojunction and bulk heterojunction.

3.5.1 Single Layer Devices

The first OSC s were based on a layer of polymer between two metal electrodes. In this structure there are only two interfaces at which excitons can dissociate. This combined with the short exciton diffusion length in polymers (around 10 nm in polyphenylenevinylene [40] and poor electron mobility [41] results in very low efficiencies, generally between 10^{-3} and 10^{-1}%.

3.5.2 Bilayer Heterojunction Devices

In a bilayer heterojunction donor and acceptor materials are stacked sequentially and sandwiched between two electrodes [37].
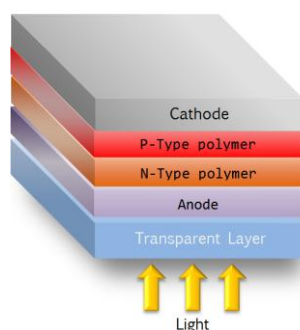
Figure 3.7 Bilayer heterojunction devices.

Charge separation occurs at the interface between the two active materials, with the highest occupied molecular orbital (HOMO) and lowest unoccupied molecular orbital (LUMO) levels of the donor higher than those of the acceptor see Figure 3.7 [42].

3.5.3 Bulk Heterojunctions

Bulk heterojunctions (BHJ) have an absorption layer mixture of a nano scale blend of donor and acceptor materials shown in Figure 3.8 The large donor-acceptor interfacial area provides in a higher possibility for the short-lived excitons to reach an interface and dissociate [43].
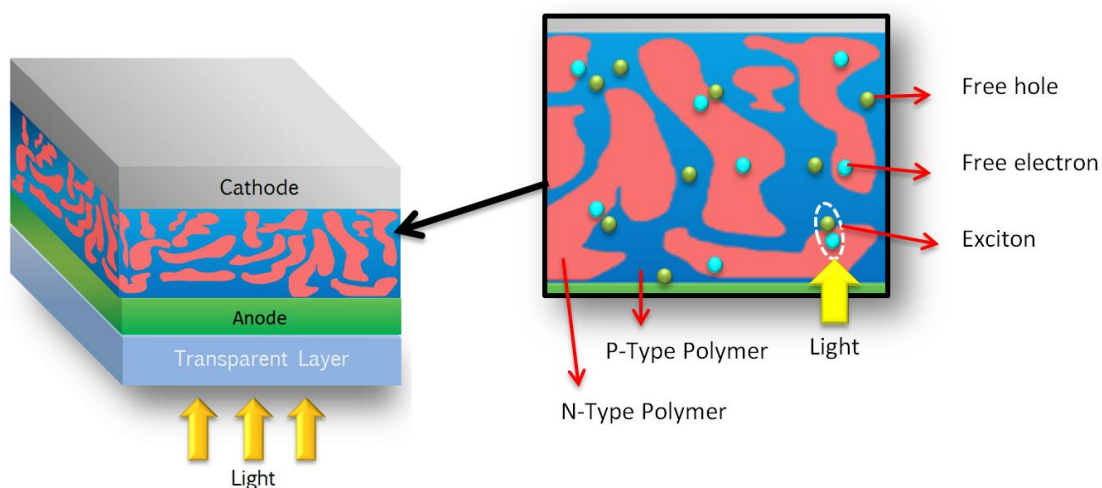
Figure 3.8 Bulk hetero junction solar cell.

BHJs have an advantage over other OSC structures due to their thick enough layer for effective photon absorption without the complex fabrication involved in oriented layer structure. BHJs can be produced by solving components in same solutions and it allows different phases of polymer to be in same medium. Different components may self-assemble into an interpenetrating network connecting the two electrodes.

Compositions are generally a polymer based donor and fullerene based acceptor. The nano structural architecture of BHJs causes difficult control, but is remarkable for

photovoltaic efficiency [44]. BHJ Solar Cells are among the most efficient solar cells that have been produced to date, with efficiencies approaching 7%.They take advantage of the increased contact area between the donor and acceptor organics. This enhances the ability for excitons to reach the donor-acceptor interface and separate before they can recombine.
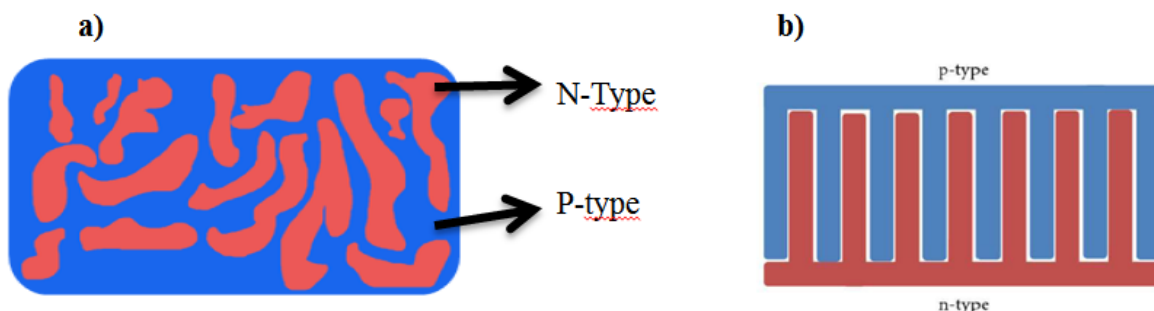
Figure 3.9 a) Schematic close up of donor-acceptor layer after being blended together to achieve its functional form. (n-type :acceptor, p-type :donor) b) Ideal structure of cell in order to maximize surface contact. The distance between materials will ideally reflect the exciton diffusion length~10nm.

In this thesis Bulk heterojunction solar cells has been studied due to the advantages over other OSC types .

CHAPTER 4

FABRICATION AND CHARACTERIZATION METHODS

4.1 INTRODUCTION

Fabrication technics are the most important part of production of an OSC. Due to the defects or contaminants, solar cell may not to work properly. From the beginning to end of fabrication process, process needs more attention. Conditions of fabrication should be prepared well and provide more efficient production. Major steps of fabrication are explained at below.

4.1.1 Cleaning

Cleaning the substrate has an important role on performance of OSC. indium tin oxide (ITO) coated glass or substrate should be cleaned with proper chemical agents. For example detergents help to remove most of organic contaminants. Also Isopropyl Alcohol and Acetone have an important role in cleaning step. All chemicals should be pure. Ultrasonic bath was our main helper device during this procedure.

4.1.2 ITO Glass Cleaning

After patterning ITO coated glass, contaminations of acids , or other compounds such as tape etc. should be removed from surface properly. Contaminants are one of the major problem sources of coatings and cell resistivities. For preventing from shorts in circuit we need to make etcing on to surface.(see Figure 4.1 After etching our pattern with HCl to the surface, respectively we followed this procedure ;

- Rinsing with pure water,
- Cleaning with detergents

- Cleaning with acetone
- Cleaning with Isopropyl alcohol.

At some cases when this procedure insufficient for removing rough contaminants, A RCA cleaning procedure can be applied.
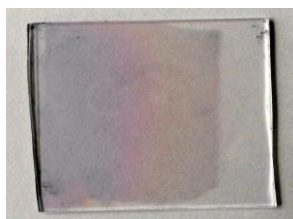
Figure 4.1 Etched ITO coated glass.

4.1.3 Spin Coating

Spin coating is a procedure used to deposit uniform thin films to flat substrates.

Figure 4.2 Spin coater device.

Usually a small amount of coating material is applied on the center of the substrate, which is either spinning at low speed or not spinning at all. The substrate is

then rotated at high speed in order to spread the coating material by centrifugal force. A machine used for spin coating is called a spin coater, or simply spinner. see Figure 4.2

Rotation is continued while the fluid spins off the edges of the substrate, until the desired thickness of the film is achieved. The applied solvent is usually volatile, and simultaneously evaporates. So, the higher the angular speed of spinning, the thinner the film. The thickness of the film also depends on the viscosity and concentration of the solution and the solvent. A widely studied phenomenon in spin-coating is the coffee ring effect (see Figure 4.3)[45].

Spin coating is widely used in micro fabrication of oxide layers using sol-gel precursors, where it can be used to create uniform thin films with nano scale thicknesses. It is used intensively in photolithography, to deposit layers of photoresist about 1 micro meter thick. Photoresist is typically spun at 20 to 80 revolutions per second for 30 to 60 seconds [46].
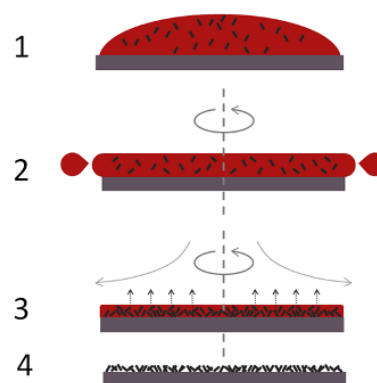
Figure 4.3 Schematic explanation of spin coating.

1. Substrate coated with desired polymer material solution by the help of pipette.
2. Substrate is rotated at desired speed which provides desired uniform thicknesses
3. Airflow during the rotation helps to evaporate the solvent in polymer.
4. Obtaining uniform polymer coating on substrate.

Solution	Rotation Speed (rpm)	Thickness (nm)
P3HT/ PCBM/ Chlorobenzene	250	110
	270	105
	300	100
	325	90
	420	**80**
	410	77
	500	65
	570	50
	660	45
	750	35
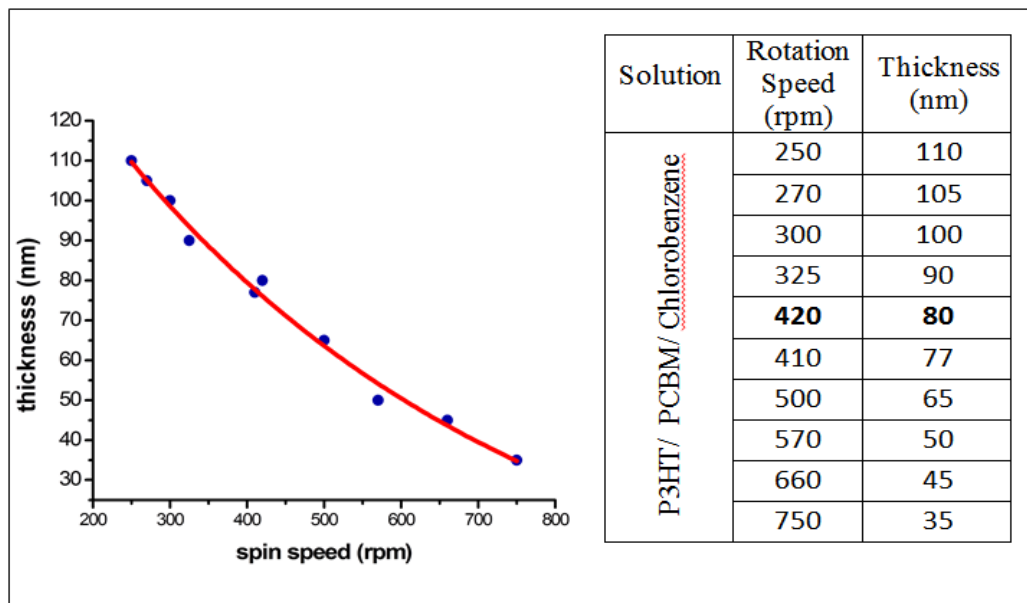
Figure 4.4 P3HT:PCBM spin coating curve.

Solution	Rotation Speed (rpm)	Thickness (nm)
PEDOT:PSS	450	115
	500	105
	570	95
	660	85
	750	75
	840	65
	930	60
	1020	55
	1110	50
	1200	**42**
	1290	40
	1380	35
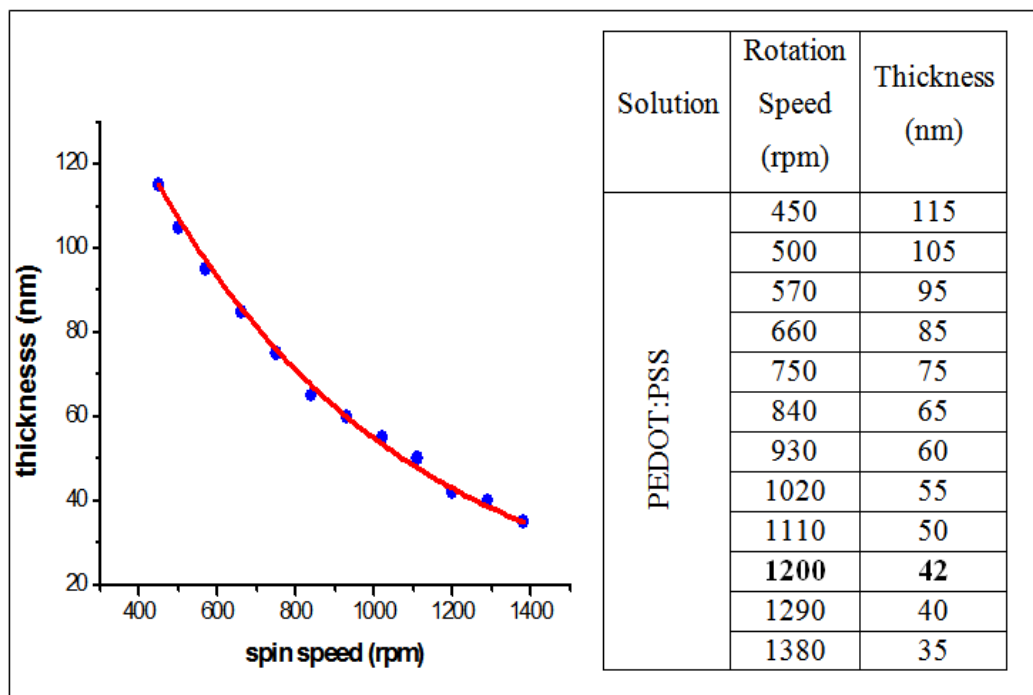
Figure 4.5 PEDOT:PSS spin coating curve.

Substrates rotation at high speed (usually > 10 rotations per second = 600 rpm) means that the centripetal force combined with the surface tension of the solution pulls

the liquid coating into an even covering. During this time the solvent then evaporates to leave the desired material on the substrate in an even covering [47]. Spin Coating parameters which are obtained in our lab, respectively on Figure 4.4-5 below. In Chapter 5 it will be explain the reasons of which conditions preferred for our OSC fabrication.

4.1.4 Annealing

Annealing is an significant part of OSC s production process. For each polymer and material type, it should be used specific annealing conditions such as temperature and time. Annealing conditions of our OSC shown in Table 4.1. In this process, repeatability is very important. Slight modifications on annealing conditions, may cause great differentiate on OSC s efficiencies. Due to this reason, annealing optimization for each layer of OSC is indispensable section of fabrication. Also equipment which use for annealing is so important. If it is possible annealing conditions of devices should be confirmed with the external devices such as thermometers etc. On the other hand Polymers interactions between each other can be possible with the appropriate thermal conditions. Mainly the annealing process, for the metals, it provides reformation of deposited atoms metal atoms on to a substrate.

Table 4.1 Annealing conditions of materials.

Material	Annealing Temp. °C	Time (min)
ITO	600	30
PEDOT:PSS	110	15
P3HT:PCBM	60	30
Aluminium	120	5

During the deposition process there may be an irregular order between metal atoms. This is causes unexpected behavior of metallic structure such as resistance, conductivity etc. A regular order of atoms minimizer those problems. For obtaining a regular order, annealing is a ideal method. For the organic materials annealing helps to

setup covalent bonds between molecules. It should be keep in mind that organic materials' structures can be damage at high temperatures. Due to this annealing process conditions should be adjust properly. Also for evaporation of organic solvents on sample, annealing process is an ideal method.

4.1.5 Magnetron Sputtering

Sputter deposition is a physical vapor deposition (PVD) method of thin film deposition by sputtering (see figure 4.5).This involves ejecting material from a "target" that is a source onto a "substrate" such as a silicon wafer. Resputtering is re-emission of the deposited material during the deposition process by ion or atom bombardment. Sputtered atoms ejected from the target have a wide energy distribution, typically up to tens of eV (100,000 K) (Figure 4.6).
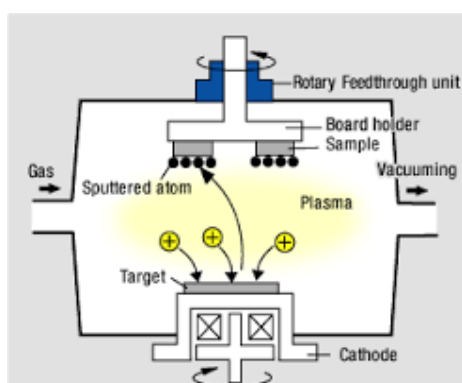
Figure 4.6 Magnetron sputter.

The sputtered ions (typically only a small fraction of the ejected particles are ionized -on the order of 1%) can ballistically fly from the target in straight lines and impact energetically on the substrates or vacuum chamber (causing resputtering). Alternatively, at higher gas pressures, the ions collide with the gas atoms that act as a moderator and move diffusively, reaching the substrates or vacuum chamber wall and condensing after undergoing a random walk.

The entire range from high-energy ballistic impact to low-energy thermalized motion is accessible by changing the background gas pressure. The sputtering gas is often an inert gas such as argon. For efficient momentum transfer, the atomic weight of the sputtering gas should be close to the atomic weight of the target, so for sputtering light elements neon is preferable, while for heavy elements krypton or xenon are used. Reactive gases can also be used to sputter compounds. The compound can be formed on the target surface, in-flight or on the substrate depending on the process parameters. The availability of many parameters that control sputter deposition make it a complex process, but also allow experts a large degree of control over the growth and microstructure of the film [48].

Table 4.2 Al coating conditions.

Coated Material	Pressure mTorr	Time min	Sputter Source	Power (watt)	Temp. °C
Aluminum	3	45	DC	30	25

During our sputtering process it is occurred that when we did not study under enough low pressure conditions, we could not able to obtain a uniform and pure surface of coating. Temperature control is also significant factor due to degradation of organic materials. For Aluminum coating we used parameters shown in table of coating.

CHAPTER 5

ITO/PEDOT:PSS/P3HT/AL LAYER ORGANIC SOLAR CELL FABRICATION

5.1 EXPERIMENTAL STUDIES

Fabrication of OSCs generally includes similarities such as spin coating; dip coating, sputter depositing etc. Minor changes of general fabricating methods find out the diversities and differences of OSC types. At the beginning of fabrication, we focus on an own OSC parameters, such as thickness, annealing conditions etc. After that, it is aimed to fabricate an optimized and repeatable OSC. Fabrication processes will be explained below.
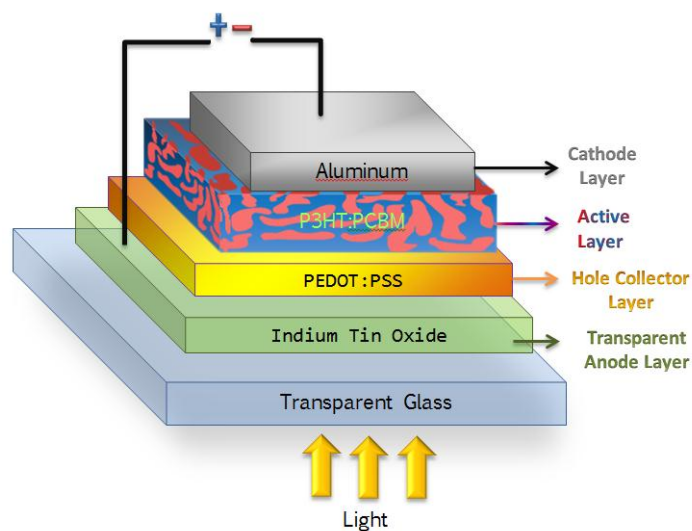
Figure 5.1 Structure of fabricated organic solar cell.

First part of experiments it has been fabricated an optimized bulk hetero junction OSC (see Figure 5.1). Due to this; standard parameters is tried to quantify and define. After supplying experimental requirements, fabrication process has been focused. As in explained at previous chapters, P3HT-PCBM and PEDOT:PSS has been used as an active layer due to the work functions (shown in Figure 5.2) and compatible fabrication technics with the devices in our research center. P3HT is p-type polymer which rich in hole. PCBM is n-type polymer which rich in electron.
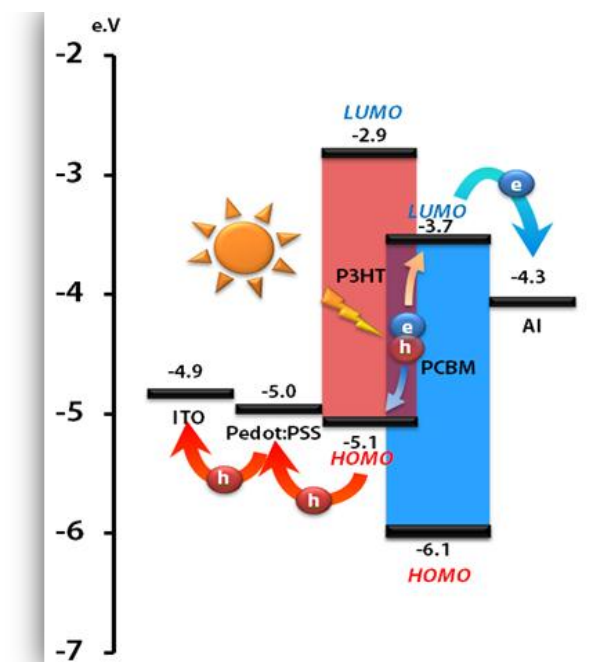
Figure 5.2 The work functions of layers.

When metals with high and low work functions are placed on each side of the organic material, they create a potential difference, which is what separates the exciton and the reason why electrons flow towards the positive electrode (cathode) and holes travel towards the negative electrode (anode). Examples of electrodes used are ITO as the anode and metals such as aluminum, calcium, or magnesium for the cathode.

5.1.1 Indium Tin Oxide Layer

ITO is widely used as transparent conducting oxides. Its major characteristics are electrical conductivity, optical transparency and the ease to be deposited as films. Ito coated glass was our choice as a transparent contact because of easy fabrication. Firstly ITO coated glass was produced in RF- DC magnetron.
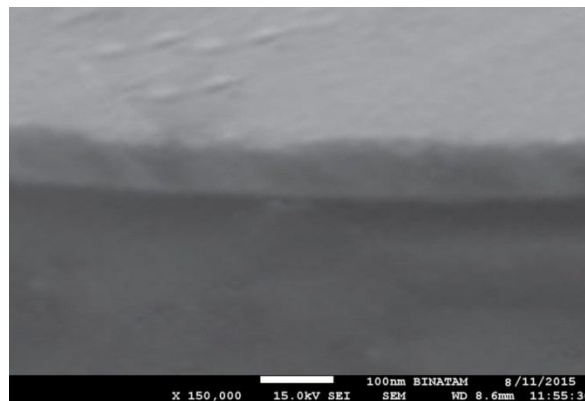
Figure 5.3 Sem image of our ITO coated glass sample.

Due to unstable results of our productions and consume of more time, ITO coated was glass supplied from Teknoma. Specifications of ITO shown in Table 5.1 and Figure 5.3

Table 5.1 ITO coated glass properties.

	Thickness	Resistivity	Transparency
ITO	110 nm	8-10 Ω/sq	%85

5.1.1.1 Removing of Indium Tin Oxide

For preventing electric short cuts it is necessary to apply etching processes on ITO surface. ITO can bond to the surface of glass firmly. For patterning ITO surface different etchants was used, such as acids. The best result that is obtained was with 37 % HCl acid solution. Treatment of ITO coated glass in HCL for 12 minutes

Table 5.2 ITO etching ratios.

Solution(%)	HCL %37	HNO$_3$	Water	Etcing Time
1.	10	10	80	25
2.	40	10	50	20
3.	60	0	40	16
4.	100	0	0	12

has provided fast, pure and certain results. Some of experiments results for this process at on Table 5.2 ITO etching ratios. For patterning process electric tape is used for covering ITO glass surface as a mask. Due to the plastic structure of tape, Acid cannot etch under covered area. After this process a cleaning process was applied to remove contaminants of tape and other organic or inorganic materials on top of ITO Coated surface (see Figure 5.4 ITO etching steps).

5.1.2 Preparation of PEDOT:PSS Solution and Coating on to ITO surface

In this processes, major problems was tried to resolve, such as cleaning of samples, preparation of solutions coating of samples and contacts' sputtering. First significant problem was, direct coating of PEDOT:PSS onto the ITO coated glass. Sigma Aldrich PEDOT:PSS (Poly (3,4-ethylenedioxythiophene)- poly (styrenesulfonate) 1.3 wt % dispersion in H2O, conductive grade.) has used [49]. PEDOT:PSS solution was sonicated minimum 45 minutes before using for preventing from particle formation of polymer. After dilutions of PEDOT:PSS : Isoprohyl Alcohol

in ratios 1:1, 2:1 ,3:1, 4:1, 5:1(ml/ml) was prepared and spin coating parameters according to 4:1 (ml/ml) PEDOT:PSS : Isoprohyl Alcohol has been optimized [50]. Isoprohyl alcohol has chosen due to be a fine organic solvent and easy to remove from medium
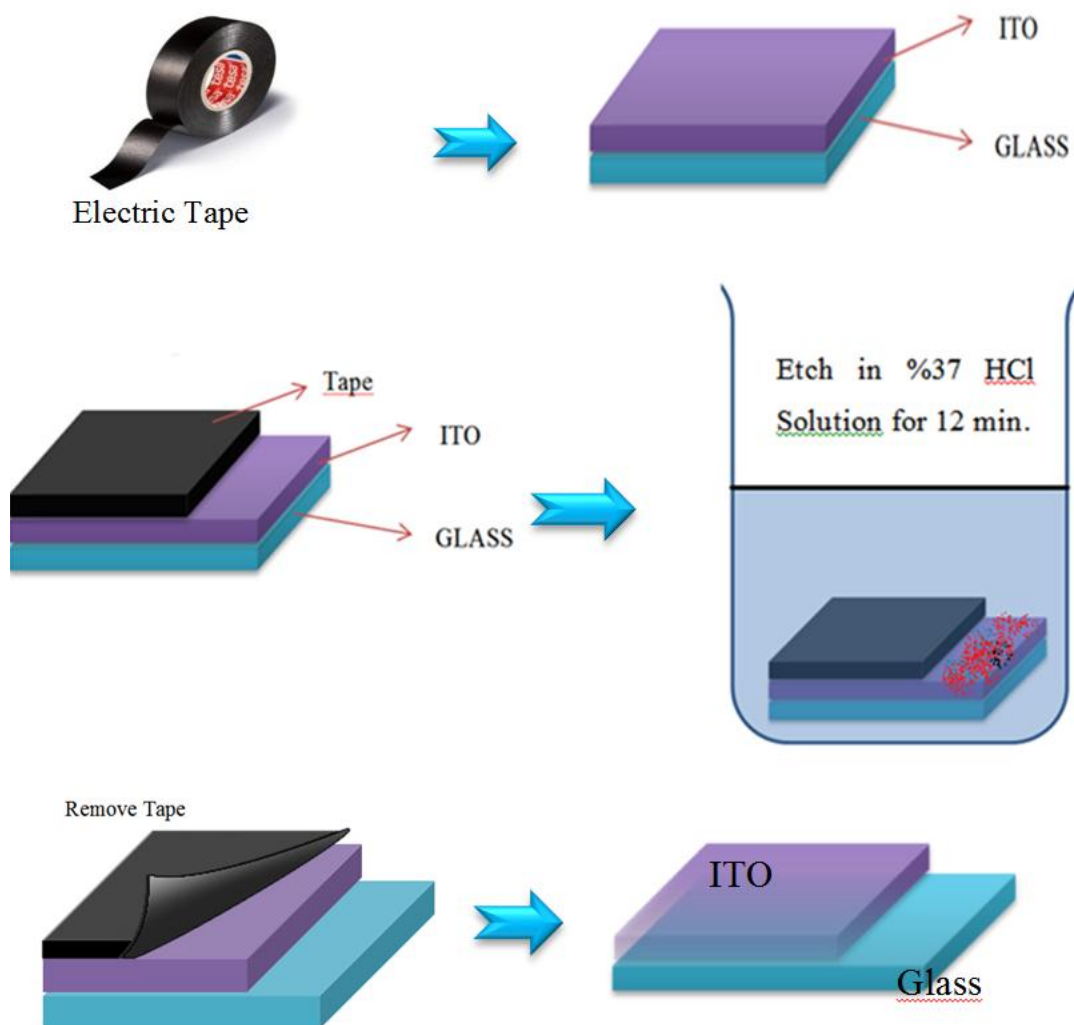
Figure 5.4 ITO etching steps.

PEDOT:PSS has a granular structure, even it solute in aqueous solutions. Due to the sonication process, if the polymer deposit directly to the surface, big particles may not allow a homogeneous coating. So that we used 0,45 µm pore sized hydrophobic syringe filter before using PEDOT:PSS. PEDOT:PSS has deposited while spin coater

started to spin. We used 5 ml syringe which is not includes rubber. Because, acidic structure of PEDOT: PSS can be react with rubber.

For coating on to the ITO coated glass we choose 1200 rpm for obtaining approximately For able to obtain desired optimum coating parameters we used 40 nm thickness of PEDOT:PSS. Than we annealed our sample in 110°C for 15 minutes for removing water on surface.

Figure 5.5 Syringe without rubber and filter.

5.1.3 Preparation of P3HT PCBM solution and coating on to PEDOT:PSS Layer

Sigma Aldrich P3HT (Poly(3-hexylthiophene-2,5-diyl)) and PCBM (6,6]-Phenyl C61 butyric acid methyl ester) is optimized for forming active layer of our OSC. For preparation precision weighing and measurements have been made. Chlorobenzene as an organic solvent of P3HT and PCBM has been used. P3HT/PCBM/Chlorobenzen in ratios of 1mg/1mg/1ml is used. After that solution is mixed via a magnetic stirrer hot plate at 50°C in 15 minutes. For coating on to the ITO coated glass 420 rpm is chosen for obtaining approximately 80 nm thickness of P3HT/PCBM. Later solar cell annealed in 60°C for 30 minutes at Nitrogen medium.

5.1.4 Aluminium Contact Layer Deposition

Vaksis RF-DC Magnetron Sputter Device (shown in Figure 5.6) has been used for depositing AL on to P3HT /PCBM layer.

Figure 5.6 RF-DC magnetron sputter device.

Deposition parameters have been optimized after several experiments.   110 nm Al has deposited At 5.1×10^{-5} mtorr , DC 30 watt , 9.5 mtorr Ar inlet, depositing 110 nm Al coating. To provide a uniform contact between Al and polymer layers, we made slow deposition within low deposition conditions such as low DC voltage and low pressure.

Figure 5.7 Result of coatings a) Slow coating of Al b) Fast coating of Al [51].

Because a non-uniform contact or in complete coverage of the metal (see Figure 5.7) over the polymer surface resulted in a scenario of charge accumulation leading to a barrier formation which explain the resulting I-V responses. After Al deposition, our sample annealed at 120 °C for 5 minutes [51]. OSC s samples which fabricated are shown in Figure 5.8.

Figure 5.8 Fabricated solar cell.

5.2 RESULTS

5.2.1 Atomic Force Microscope (AFM) Measurements

AFM or scanning force microscopy (SFM) is a very high-resolution type of scanning probe microscopy (SPM), with demonstrated resolution on the order of fractions of a nanometer, more than 1000 times better than the optical diffraction limit.

File Name	2 Topog...phy 793 cropped
Head Mode	NC-AFM
Source	Topography
Data Width	256 (pxl)
Data Height	246 (pxl)
X Scan Size	40 (µm)
Y Scan Size	38.44 (µm)
Scan Rate	0.5 (Hz)
Z Servo Gain	1
Set Point	8E-3 (µm)
Amplitude	19.199E-3 (µm)
Sel. Frequency	295.12E3 (Hz)
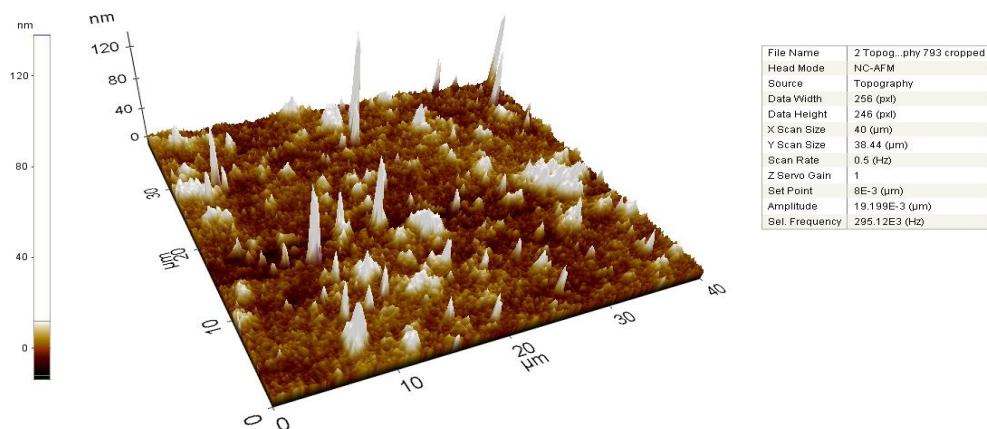
Figure 5.9 PEDOT:PSS layer topography.

The AFM consists of a cantilever with a sharp tip (probe) at its end that is used to scan the specimen surface.

File Name	2 Topog...phy 793 cropped
Head Mode	NC-AFM
Source	Topography
Data Width	250 (pxl)
Data Height	164 (pxl)
X Scan Size	39.06 (µm)
Y Scan Size	25.62 (µm)
Scan Rate	0.5 (Hz)
Z Servo Gain	1
Set Point	8E-3 (µm)
Amplitude	19.199E-3 (µm)
Sel. Frequency	295.12E3 (Hz)
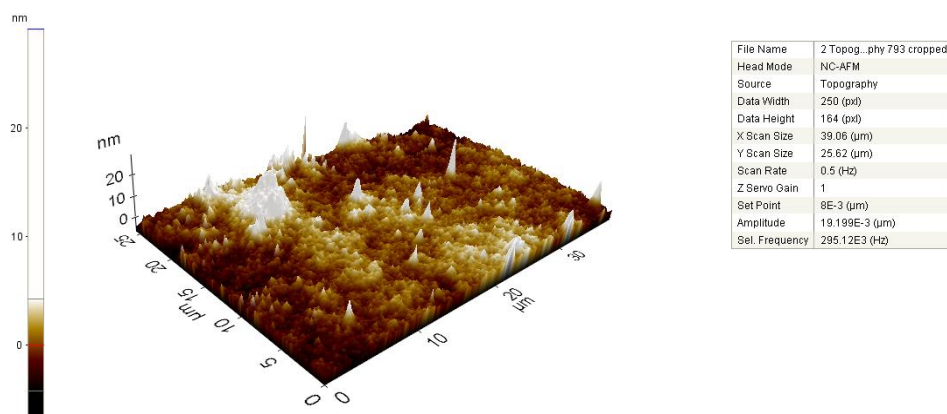
Figure 5.10 AFM images of P3HT PCBM layer.

The cantilever is typically silicon or silicon nitride with a tip radius of curvature on the order of nanometers. When the tip is brought into proximity of a sample surface, forces between the tip and the sample lead to a deflection of the cantilever according to Hooke's law [52]. PEDOT:PSS and P3HT-PCBM layers of OSC has been monitorized within AFM (shown in Figure 5.9, Figure 5.10). Non-contact mode used due not to damage the surface of layers.

5.2.2 Current-Voltage Characteristics

Fabricated OSC current voltage relations are shown in below. At solar cell physics, P-N junction formation is significant factor which affects parameters of OSC.

Table 5.3 I-V Characteristics of organic solar cells.

Sample	Voc (V)	Jsc (mA /cm^2)	Pmax mW/cm^2	Fiil Factor FF%	Power Conversion Efficiency (PCE) %	Rsh (mOhm cm^2)	Rs (mOhm cm^2)
Osc 1	0,57	0,5200	0,107	35	0,001	5,39	0,853
Osc 2	0,55	1,0600	0,225	38	0,002	1,66	0,432
Osc 3	0,52	0,3700	0,063	32	0,063	1,07	2,890
Osc 4	0,5	0,9800	0,153	31	0,150	0,96	0,313
Osc 5	0,5	0,4900	0,106	43	0,430	4,45	0,450
Osc 6	0,5	0,0016	0,031	38	0,031	14,29	4,202
Osc 7	0,34	0,1230	0,009	21	0,009	2,20	3,788
Osc 8	0,5	0,2100	0,022	21	0,022	2,13	2,506
Osc 9	0,5	0,3630	0,041	22	0,040	1,43	1,818
Osc 10	0,53	0,7131	0,080	21	0,080	0,68	1,935
Osc 11	0,55	0,0069	0,001	26	0,100	1,79	0,704
Osc 12	0,58	4,9600	0,940	32	0,940	0,46	0,096
Osc 13	0,53	6,0948	1,191	36	1,191	0,27	0,059
Osc 14	0,48	0,2955	0,045	31	0,045	3,36	2,045
Osc 15	0,56	4,4245	0,962	38	0,962	0,50	0,122

Even positive improvements in P-N junction formation, our samples' solar cell characteristic has been increased by differentiation on PCE [53,54,55] . In order to define PCE, series resistance (Rs) and Shunt Resistances (Rsh), we measured the current-voltage characteristics by using a Keithley 4200-Semiconductor Characterization System. Series resistances were then extracted from the dark I–V measurements (shown in Table 5.3 and Figure 5.11).

The major fact that affects our study was, annealing of each layer. It is observed a remarkable relation between solar cell efficient and annealing conditions (Shown in table 5.4). Series resistance is another significant parameter for OSC s.
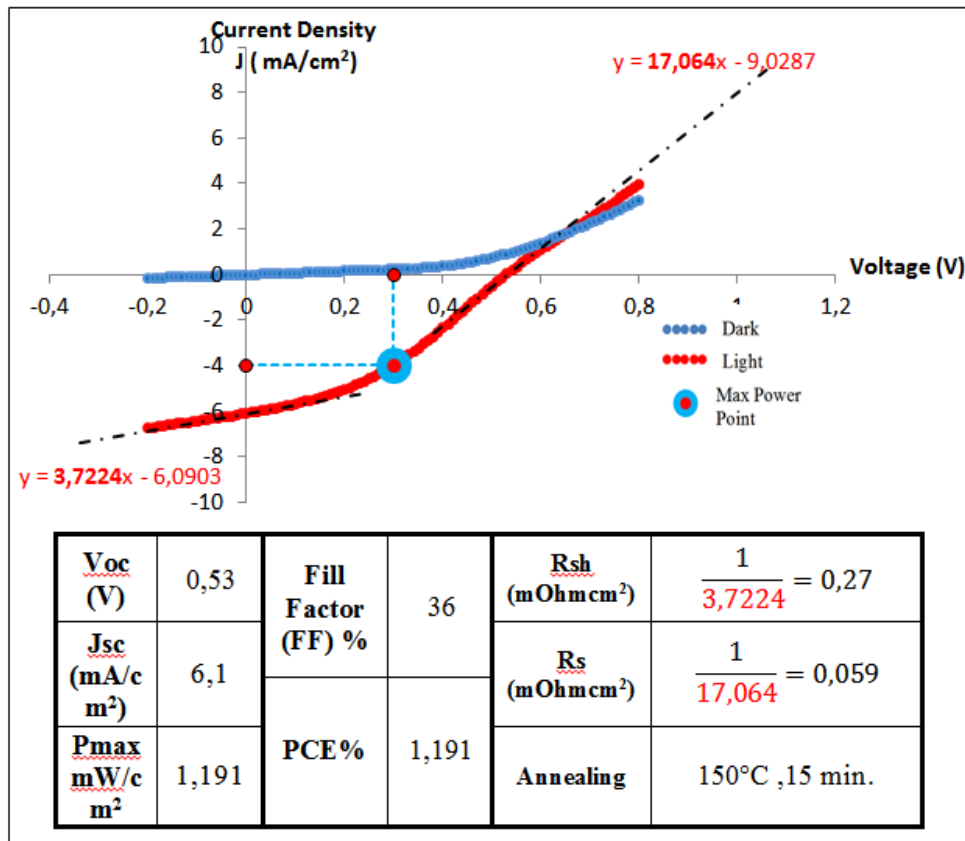
Figure 5.11 OSC13 J-V measurements.

Blue curves on figure belong to J-V behavior under dark (no illumination). Red curve represent J-V differentiation under light conditions of 1000 W/m2 air mass 1.5 global (AM 1.5 G) illumination. Rsh and Rs are calculated under illumination.

By fabricating OSC devices with different active layer thicknesses, a relationship of the series resistance with thickness can be established from which bulk and contact resistances were derived. It is also known that a high series resistance reduces the fill factor and cell efficiency (see Table 5.4). Rsh and Rs is calculated under illumination .Rsh calculated from the left of the J-V curve's tendency and Rs is calculated from the right of the J-V curves' tendency. Red color written equations In figure 5.10 help us to define tendencies of J-V curvature at point of Isc (V=0) and Voc (J=0). Annealing conditions also studied for the same type of OSC samples.

Table 5.4 Changes of PCE at different annealing conditions.

Sample	Power Conversion Efficiency (PCE) %	Rsh (mOhm) cm^2)	Rs (mOhm) cm^2)	P3HT/PCBM/Al Annealing	
				Temp. (°C)	Time (Min)
Osc 1	0,001067	5,393743	0,852806	150	15
Osc 3	0,063	1,07	2,890	150	10
Osc 7	0,008842	2,20022	3,787879	120	15
Osc 8	0,022336	2,131287	2,505638	120	10
Osc 11	0,09998	1,785714	0,704225	75	10
Osc 12	0,94000	0,462449	0,096432	60	30
Osc 13	1,190639	0,268644	0,058603	60	30

For each annealing time and temperature, same ratios of materials have been used during the fabrication. It is tried to decrease shunt resistance (Rsh) and series resistance (Rs) by using different mixture ratios.

CHAPTER 6

GOLD NANO PARTICLE DOPED ORGANIC SOLAR CELL FABRICATION

6.1 INTRODUCTION

Light trapping has an important role in solar cell field due to provide an improved absorption by using of metal based nanoparticle additions to the solar cell structure. plasmonic and organic photovoltaic field researchers are in a spirit to enhance the sun light absorption and electron –photon coupling for increasing the photo voltaic devices. In OSC s, the photovoltaic conversion efficiency is closely connected with absorption of incident light and collecting opposite charges at opposite electrodes [56].

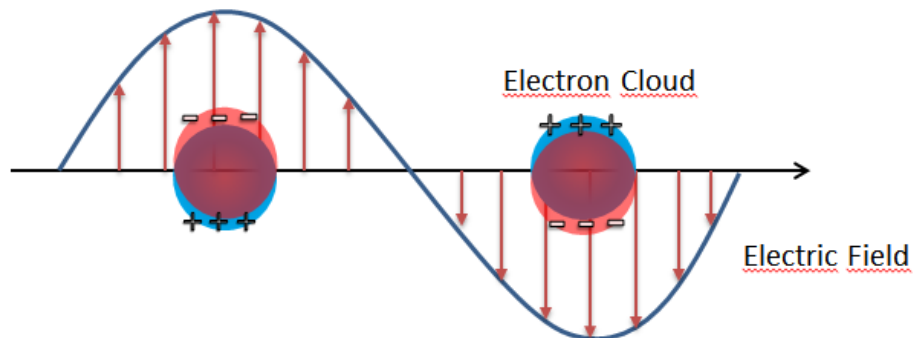Figure 6.1 Surface resonance plazmon in oscillations of strong interactions of metal nano aprticles and free electrons by incident radiation[58].

Trapping of light in OSC s is a method which contributes of incensement to the power conversion efficiency in OSC devices similarly to what was carried out with known thin film silicon solar cell technology within the thickness of the silicon is about

a few micrometers [57]. Even metallic particles are in same analogy or lower size than the wavelength of the incident light of interest, between the electromagnetic radiation and between the free conduction electrons of metal atoms a powerful interaction forms.

In metallic structures free electrons generates a dipole into the particles. After the interaction of that electrons and incident light , Plasmons are formed which are oscillations (see

Figure 6.1).   Even the electrons' oscillation resonance suits or matches with the incident light frequency the resonance conduction occurs . This is also called as localized surface plasmon resonance which can be applicable for nano structures.

The energy of plasmon in a free electron defined as [58];

$$Ep = \hbar \sqrt{\frac{ne^2}{m\varepsilon_0}} = \hbar\omega_p \tag{6.1}$$

Where

n :   Density of free electrons

e   Elementary charge

ε_0 Permittivity of free space,

m   Mass of electron

$\hbar$ Planck constant

ω_p Plasmon frequency of bulk.

The dielectric function for metals with low interband absorption can be described with the Drude model, which explains the damp response, with a frequency of ω ,free electrons to an applied electromagnetic field with a frequency of ω

$$\varepsilon_r(\omega) = 1 - \frac{\omega_p}{\omega^2 + i\gamma\omega} \tag{6.2}$$

Where

$\tau = \dfrac{1}{\gamma}$ Relaxation time

ω   Angular frequency of an applied electromagnetic field.

Even a metallic nano particle stated in same kind medium, this structure can allow the light scatter in both up and down directions. Alternatively, the scattering of light will into more the dielectric with larger the ability of a substance to store electrical energy in an electric field.[59-60]. Instead, the light will scatter more into the dielectric with larger permittivity.
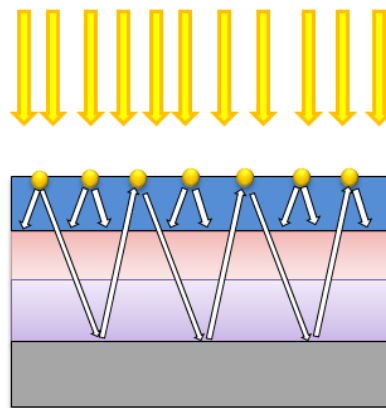
Figure 6.2 Light scatter in solar cell.

Another possibility is fitting of nano particles between two dielectric interface. At this time it is probable to increase the optical path length by lights' angular spread in dielectric medium [61]. For the multiple scatterings, the metal contact show a reflecting behavior toward the surface and this is resulting multiple light scatterings and passes over the OSC s (shown Figure 6.2).

In electromagnetic studies field the absorption and scattering can be explained. In electromagnetic field, when the diameters of metal nanoparticles lower than the lights'

wavelength, The absorption and scattering mechanism can be explained with a dipol moment.

The cross-section of light scattering and absorption are given H. Bohren;

$$C_{scat} \frac{1}{6\pi} \left(\frac{2\pi}{\lambda}\right)^4 |\alpha|^2 \qquad ; C_{abs} \quad \left(\frac{2\pi}{\lambda}\right) \text{lm}[\alpha] \qquad (6.3)$$

With

$$\alpha = 3V \frac{\omega_p^2}{\omega_p^2 - 3\omega^2 - i\gamma\omega} = 3V \left[\frac{\frac{\varepsilon_p}{\varepsilon_m} - 1}{\frac{\varepsilon_p}{\varepsilon_m} 21}\right] \qquad (6.4)$$

α :   Particle polarizability,

V: The volume of particle,

ε_p :   Tthe particle dielectric function

ε_m: Dielectric function in medium

If ε_p=-2ε_m the polarizability of particle will be larger [55].
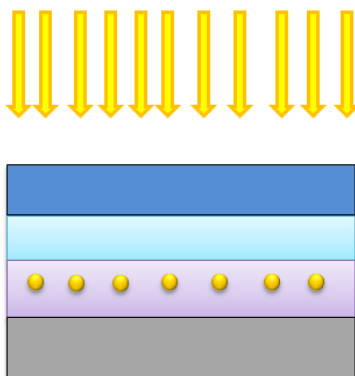
Figure 6.3 Gold NPs between active layers.

When it concerned about spherical structure, the surface plasmon is given by;

$$\omega_{sp} = \sqrt{3\omega_p} \tag{6.5}$$

The efficiency of scattering occurs at [55]:

$$Q_{scat} = C_{scat}/(C_{scat} + C_{abs}) \tag{6.6}$$

In OSC it is possible to take an advantage from resonant Plasmon of the highly local field increases on all sides of the metallic nanoparticles causes to the increases the absorption of light surround of area (see Figure 6.3).

Figure 6.4 Gold nanoparticle charge distribution and plasmon resonance and for near field distributions for the vertically Transverse polarization with incident light in P3HT:PCBM.

Gold nanoparticles can behave as antennas by having closest size of the light wavelength for enhancement of incident light density. This electric field enhancement can be more than 100 times of normal light behavior. [63].

Plasmonic studies results that when Au nano particles embedded into the active layer ,a following effect, light absorption enhancement occurs. (see Figure 6.4) [64].
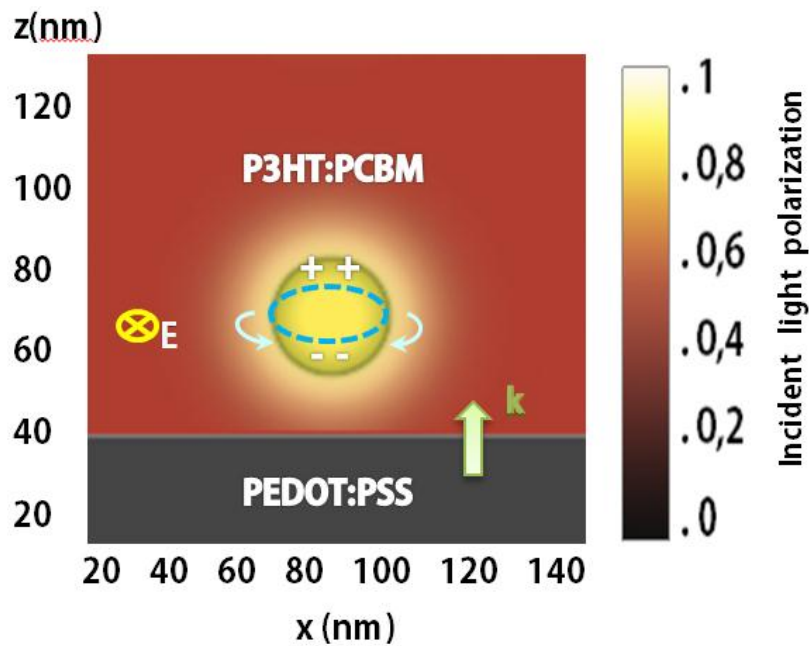
Metals which chose for using in OSC s generally have an strong interaction with light. Gold, Aluminum, lead are some of those.

Especially the surface plasmon resonance is caused by aluminum and silver in UV spectrum. On the other hand in visible spectrum, gold and copper directs the surface plasmon resonance.[63].
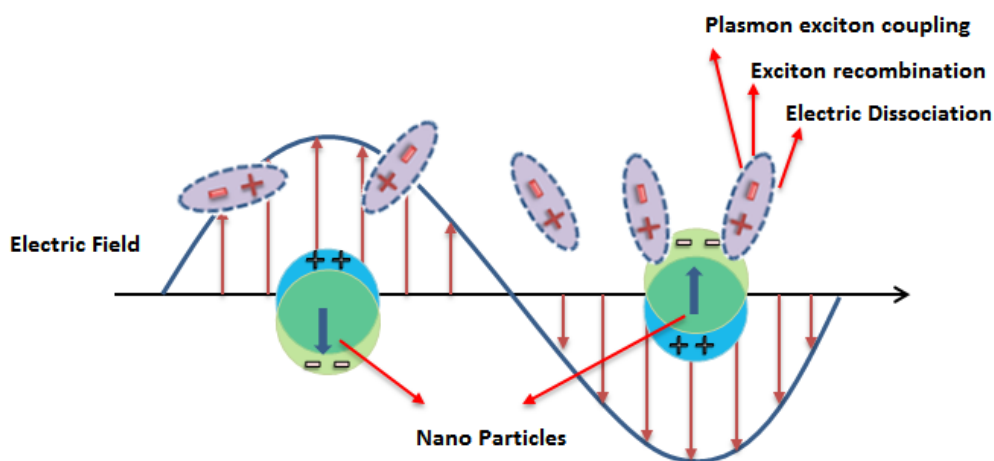
Figure 6.5 Excitons and localized surface plasmon resonans interaction. This interaction decreases exiton recombination and increases exiton dissociation [65].

The properties of metals are important. silver may preferred due to its lower prices and low light absorption but oxidation is another obstacle for production. Due to this, Studies widely focused on gold nano particles. Also unluckily clusters of gold may behave a exotermic absorber of O_2 (see Figure 6.5)

6.2 EXPERIMENTAL STUDIES

6.2.1 Gold Nanoparticles Synthesis for Organic Solar Cells

Gold nanoparticles are able to produce with different methods such that liquid ablation within laser and chemical production methods, [66] and respectively gold nanoparticles can deposit on a substrate and it can be followed with thermal annealing [67].

Chemically Gold nanoparticles can be produced by the reduction of a molecule which is precursor. Halide variants of gold are common precursors. These precursors are prepared by solving of bulk gold in aqueous solution or metal cyanide with gold chloride ($AuCl_3$). or variations. The chemical reactions should be done under controlled and reducing agents should be added to the solution which prepared with precursor. Reducing agent distribution affects the distribution and size of synthesized nanoparticles. Size distribution is also depends on concentration of solution, time of aging, and technique of reduction. .The citrate reduction reaction is one of the most known methods for synthesizing is spherical Gold nanoparticles with Turkevich method.
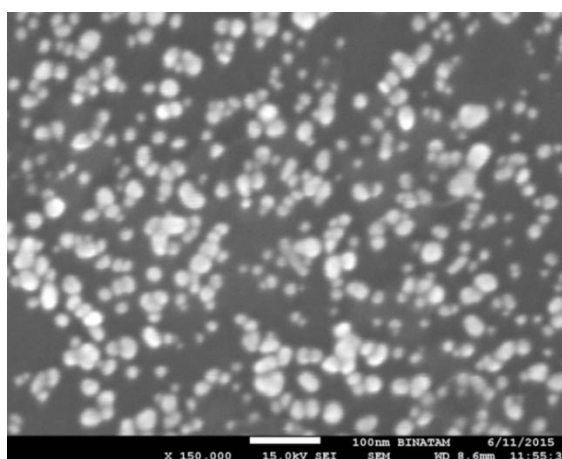
Figure 6.6 Au Nanodot SEM images.

Gold Nano particles have been synthesized by liquid chemical method by using (HAuCl4) and NaBH4. NaBH4 is a powerful reducing agent. So Au element in HAuCl4 compound can be reduced easily with titration by controlling reaction conditions such as Heat and stirring speeds. Reaction equation is shown at below.

$$HAuCl_4 + NaBH_4 \rightarrow Au + B(OH)_3 + NaCl + H^+ \tag{6.7}$$

Nano size control of Au atoms is possible with tuning heating conditions. Aggregation of atoms occurs by heat increases. Sem analyses images of our liquid gold nano particle solutions shown in Figure 6.6.

6.2.2 Dopping of Au nanoparticles On to Ito Layer

We used two different methods to nano gold dopping between OSC layers. Firstly, we coated liquid Au nano particle solution on to ITO layer. Than substrate heated for evaporating liquid than normal OSC production procedures which explained in Chapter 5 is being followed. Au nano dot on to ITO layer is analyzed via scanning electron microscope (SEM) (see Figure 6.7).
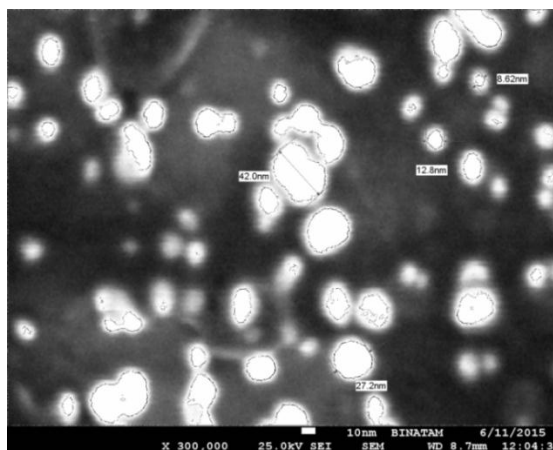
Figure 6.7 Au nanodot coated ITO suface.

Secondly we used RF-DC magnetron to coat Au nanodot on to ITO layer. Firstly our ITO surface of sample is coated with Au layer approximately 5 nm.. After that;

substrate annealed at 600° C for 30 minutes for collaboration of nanogold layer as nanodot. For understanding the changes of solar cells, two different solar cell fabricated which includes Au nano dots and without Au nano dot. Results are shown in Figure 6.8 and Figure 6.9.

Voc (V)	0,53	Fill Factor (FF) %	36	Rsh (mOhmcm^2)	$\frac{1}{3,7224} = 0,27$
Jsc (mA/cm^2)	6,1			Rs (mOhmcm^2)	$\frac{1}{17,064} = 0,059$
Pmax mW/cm^2	1,191	PCE%	1,191	Annealing	150°C ,15 min.

Figure 6.8 OSC without nanoparticles.

Figure 6.9 OSC which is included Au nanoparticles which doped with liquid Au solution.
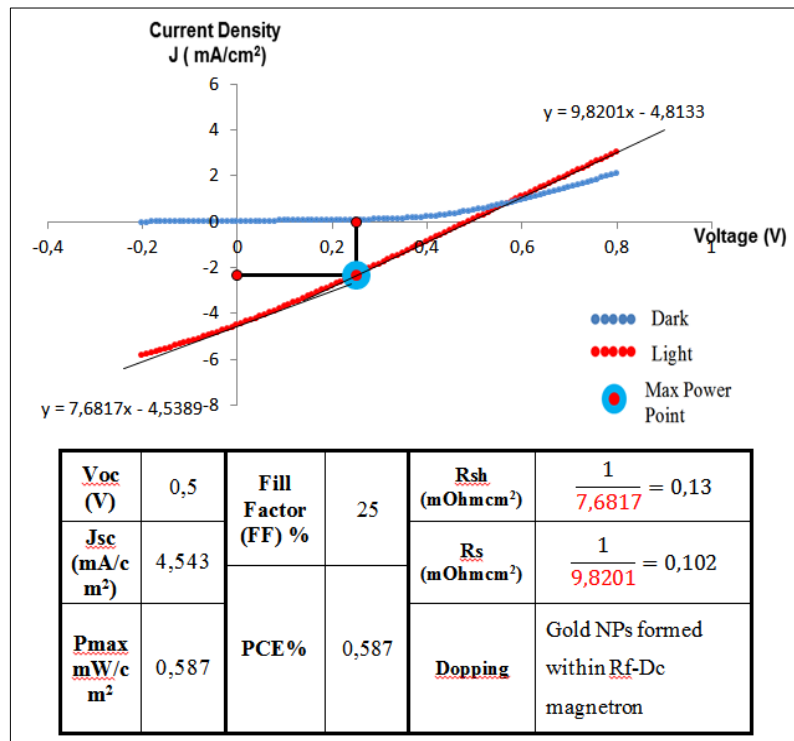
Figure 6.10 OSC which is included Au nanoparticles which doped RF-DC magnetron.

CHAPTER 7

CONCLUSION

7.1 SUMMARY OF STUDY

In this thesis, Al/P3HT:PCBM/ PEDOT:PSS/ITO bulk heterojunction OSC and Isc=6.09 mA and Voc= 0,53 and PCE %1.19 was the max obtained values of our standard fabricated OSC. PEDOT:PSS used as an electron blocking layer or hole injector, ITO used as an Anode and Aluminum used as an cathode layer due to work function and HOMO-LUMO properties.
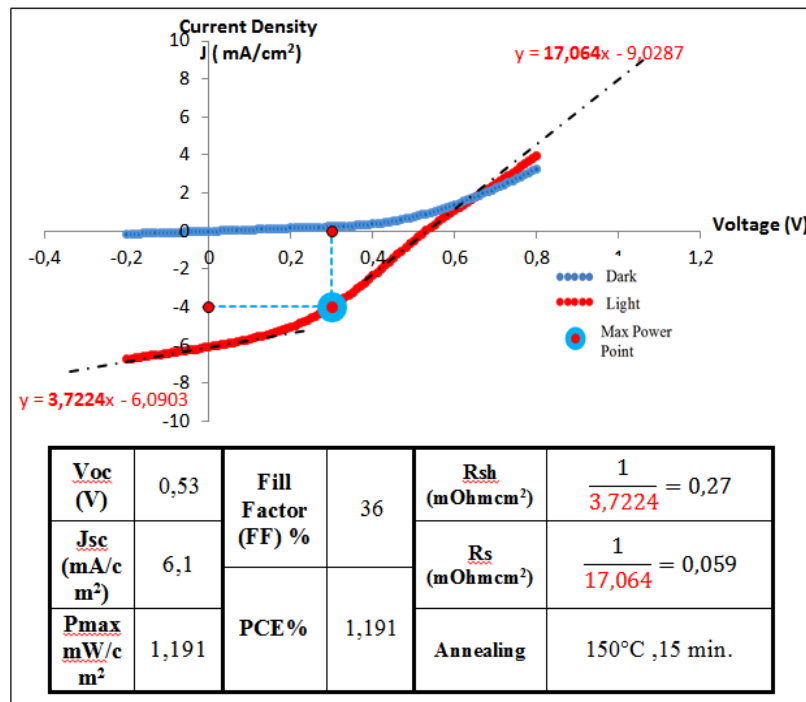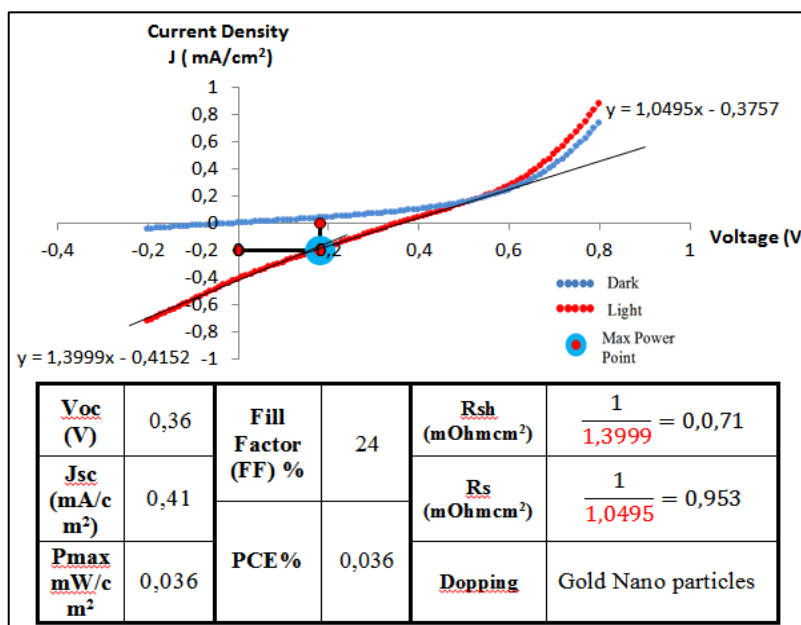
Gold nano particles (NP) doped OSC has been fabricated with two different Nano dot production methods operated As a NP we used Gold Nano dots which formed via RF-DC magnetron sputter device and aqueous solution of gold NPs. By RF-DC magnetron device gold NP; I_{SC} =4,5438, V_{OC}=0.5, PCE %=0.587 and by aqueous solution of gold NPs; I_{SC}= 0.4142 mA V_{OC} 0.36 V and PCE % =0,036 values measured under .A.M. 1.5 G illumination condition via halogen light source and Keithley 4200-semiconductor characterization system has been used for OSC characterization.

Firstly ITO layer tried to coat on to glass via RF-DC magnetron sputter device. RF mode has been chosen due to the voltage ramp control. It is observed that with in direct high voltages can leads to damage on the structure of ITO target. For obtaining a homogeneous   coating   substrate   glass   continuously   rotated   at   10

rpm. By using 5 minutes ramp 50 watt applied to ITO source and in 5×10^{-5} Mtorr pressure for 30 minutes in RF mode ITO coated on to glass substrate. Morphology of ITO coated glass surface has been investigated via AFM and SEM. Approximately 110 nm ITO coating has been 30 ohm/sq resistance measured on coated substrate. But it is observed that disorders on ITO surface lead to surface resistance differences To obtain regular coating structure we supplied same conditioned ITO coated glass from private company. ITO has been used as an anode layer. For preventing shorts we decided to etch a fragment of ITO on surface. For etching our pattern on to ITO we applied HCl (%37) for 12 minutes. More than this time limit leads to over etching under covered parts. Before starting deposit other organic compounds, ITO coated glass has been cleaned within detergents and pure water.

PEDOT:PSS has been ordered from Sigma Aldrich. It is used as a hole collector layer in our OSC Solution has been prepared by diluting PEDOT:PSS with Isopropyl Alcohol in ratios 5:1 and sonicated for 45 minutes for solving PEDOT:PSS particles. Spin coating method used for covering PEDOT:PSS due to obtain an pure and uniform surface. After coating, to remove solvents (water ,isopropyl alcohol) , substrate has been heated or annealed on 110 $^{\circ}$C for 15 minutes .It is observed that above this temperature conditions, PEDOT:PSS structure can be damage and below this temperature it takes longer to remove the solvent of PEDOT:PSS solution. 40 nm thickness obtained after coating procedure. AFM and SEM used to measure thicknesses.

P3HT and PCBM have been chosen as an active layer due to defined stabile performance specification on literature and marketing.P3HT and PCBM has been supplied from Sigma Aldrich. It is tried to obtain approximately 80 nm active layer .Due to this after several experiments and tries polymer solution has been prepared with P3HT/PCBM/Chlorobenzen in ratios of 1mg/1mg/1ml . Spin coating method used for covering P3HT/PCBM/Chlorobenzen due to obtain a pure and uniform coating. After coating, substrate annealed in 60°C for 30 minutes with in nitrogen flow due to establish a stable structure and remove solvents (Chlorobenzene etc.) from substrate. It is investigated that more than 60°C temperatures, active layer starts to lose structural stability and electrical functions. AFM and SEM used to measure thicknesses. For obtaining a uniform coating and to obtain a thickness less than ITO layers' we decided

to gain approximately 60 nm thickness. For this thickness we spin coated at 1200 rpm for 40 second.

Aluminum deposition has been made on RF-DC magnetron device in DC Mode. For obtaining a uniform and ideal contact to active layer, 30 watt applied to Al target. deposition has been made at low voltage. Sample stage has rotated at 7 rpm during procedure. For preventing from oxide layer which blocks electron transfer from active layer, Sputter pressure adjusted 6×10^{-6} mTorr. Deposition continued for 50 minutes. After procedure 100 nm Aluminum thickness obtained. Thicknesses characterized via AFM.

First type of Gold ND production via RF-DC magnetron has been on to ITO coated layer. After coating 5 nm gold, for forming gold NDs, surface has been heated to 600 °C in nitrogen medium for 1 hour. Second type of dopping has been made by coaing Gold NPs aqueous solution via Spin coater. Then substrate annealed for removing aqueous solution. For each these two type gold ND doppings PEDOT:PSS/P3HT:PCBM/Aluminum deposition has been followed. Characterization of NDs' has monitored via SEM.

For All those OSC layers preparations, importance of annealing time and temperatures has been investigated. It is observed that at high annealing temperatures, OSCs' series resistance and shunt resistances has been increased.

7.2 RESULT AND DISCUSSION

ITO/PEDOT:PSS/P3HT:PCBM/Al OSC structure and Gold NP. doped OSC has successfully investigated and fabricated%1,19 efficiency achieved with. Normal OSC, and %0,58 efficiency has achieved by Golp Nano material addition.

During fabrication it is observed that cleaning, annealing, spin Coating and sputtering steps should be done precisely due to influence of OSC efficiencies. It is observed that Rs and R_{SH} directly affected by all fabrication process steps.

At first step, ITO surface, might have a pure contact layer to provide a well holding surface to the PEDOT: PSS. It is achieved by cleaning ITO surface with cleaning detergents and organic solvents. Then as a good surfactant, Isoprophyl alcohol applied to the ITO surface and succeeds. It is detected that some organic solvents such as acetone leaves residual contaminants on ITO surface. For having an efficient OSC, this step should be considered.

PEDOT:PSS sonicated at least 45 minutes before use due to prevent of aggregation of polymer particles. After that, before filtering solution, an dilution has been done with Isoprohyl alcohol for adjusting a compatible solution with spin coater parameter.

P3HT:PCBM layer could be able to deposit on to PEDOT:PSS by solving into the chlorobenzene solution in defined ratios. It is observed that P3HT:PCBM solution should not prepare more than 70 °C. After this temperature, characteristic behaviors of polymers started to change from desired. For each solution, clean pipettes and tubes used for preventing from contaminations.

Aluminum deposition was another part of fabrication. As a contact layer Al has been chosen and a coating of Al has done via RF-DC sputter. It is observed that a precise coating should be done under low pressure to prevent from oxidation of Aluminum. It is viewed that oxidized Aluminum show a darker color than grey. Another parameter was coating speed. Desired contact effect has been achieved under low pressure and low voltages. Due to sustain this, Coating is done more than 40 minutes. To obtain desired thickness we demonstrated that 55 minutes was suitable for our desired layer thicknesses. Also for reduce the series resistance; high quality (small sized) aluminum deposition should be done precisely. This was provided more current to our cell.

Annealing was our last and most important part of production. For each step, annealing have a significant role and directly affect P-N contacts and contacts between anode, cathode and active layers. Without annealing production is impossible but at high temperatures annealing heat also do not let to fabricate an efficient OSC. From the beginning to end of fabricating, each steps of layer production also need specific annealing conditions. Respectively for ITO 600°C 30 min, for PEDOT:PSS 110

°C 15 min, for P3HT:PCBM 60°C 30 and for Al 120 °C 5 min applied and successfully OSCs fabricated.

°C 15 min, for P3HT:PCBM 60°C 30 and for Al 120 °C 5 min applied and successfully OSCs fabricated.

REFERENCES

[1] Goldemberg, J., "The promise of clean energy", Energy Policy, Vol. 34, pp. 2185–2190, 2006.

[2] Chedid, R., Kobrosly,M. and Ghajar, R., "A supply model for crude oil and natural gas in the Middle East", Energy Policy, Vol. 35, pp. 2096–2109, 2007.

[3] Kroon J. M. M., Wienk, M., Verhees, W. J. H. and Hummelen, J. C., "Accurate efficiency determination and stability studies of conjugated polymer/fullerene solar cells", Thin Solid Films, Vol. 403, pp. 223, 2002.

[4] Shaheen, S. E., Brabec, C. J., Sariciftci, N. S., Padinger F., Fromherz, T., and Hummelen, J. C., "2.5% efficient organic plastic solar cells", Applied Physics Letters, Vol. 78, pp. 841, 2001.

[5] Moldovan M. D., Visa I., Neagoe M. and Bogdan G. "Solar Heating & Cooling Energy Mixes to Transform Low Energy Buildings in Nearly Zero Energy Buildings" Energy Procedia, Vol. 48, pp. 924–937, 2014.

[6] Brabec, C.J., "Organic photovoltaics: Technology and market", Solar Energy Materials and Solar Cells", Vol. 83, pp. 273-292, 2004.

[7] Martin A., Green Solar Cells Operating Principles, Technology, And System Applications, Prentice Hall, California, 1981.

[8] Kim, Y., Choulis, S. A., Nelson J., Bradley D. D. C.,Cook, S. and Durrant J. R., "Device annealing effect in organic solar cells with blends of regioregular poly(3-hexylthiophene) and soluble fullerene", Applied Physics Letters, Vol. 86, 2005.

[9] Krebs F.C., Norrman K., "Analysis of the Failure Mechanism for a Stable Organic Photovoltaic During 10 000h of Testing", Progress In Photovoltaics: Research And.
Applications. Vol.15, pp.697, 2007.[10] Fraas L. and Partain L., Solar Cells And Their Applications, Wiley, Texas,2007

[11] Ashok S., "Solar cell" Encyclopedia Britannica, 2014.
http://www.britannica.com/EBchecked/topic/552875/solar-cell/45872/Development-of-solar-cells

[12] Conibeer, G., "Third-generation photovoltaics" Materials Today", Vol. 10, pp. 42-49, 2007.

[13] Scharber, M.C. and Sariciftci, N.S., " Efficiency of bulk-heterojunction organic solar cells" Progress in Polymer Science, Vol. 38, pp. 12, 2013,

[14] Krebs et. al., "Freely available OPV—The fast way to progress", Progress in Polymer Science, Vol. 1, pp. 378-381, 2013.

[15] Pagliaro M., Palmisano G. and Ciriminna R., Flexible Solar Cells, Wiley, Weinheim,2008.

[16] Hall, C., Tharakan, P., Hallock, J., Cleveland, C. and Jefferson, M., "Hydrocarbons and the Evolution of Human Culture." Nature, Vol, 426 pp. 318, 2003.

[17] Nelson, J., The Physics of Solar Cell, Imperial College Press, London, 2003.

[18] Liang, W Y (1970). "Excitons". Physics Education, 1970.

[19] Gevorgyan S.A., Production, Characterization and Stability of Organic Solar Cell Devices, Ph.D. Thesis, Risø DTU National Laboratory for Sustainable Energy, 2010.

[20] Petritsch, K., Organic Solar Cell Architectures, Ph.D. Thesis, Graz Technic University, 2010.

[21] Wikipedia, Solar cells, 2015.
http://en.wikipedia.org/wiki/Theory_of_solar_cells

[22] Shrotriya, V., Li, G., Yao, Y., Moriarty, T., Emery, K. and Yang, Y. "Accurate measurement and characterization of organic solar cells", Advanced Functional Materials, Vol. 16, pp. 2016-2023, 2006.

[23] American Society for Testing and Materials, Reference Solar Spectral Irradiance: Air Mass 1.5, 2015.
http://rredc.nrel.gov/solar/spectra/am1.5/

[24] International Energy Agency, Solar Photovoltaic Energy, 2010.
http://www.oecd-ilibrary.org/content/book/9789264088047-en

[25] Zabihi, F., Xie. Y., Gao, S. and Eslamian, M., "Morphology, conductivity, and wetting characteristics of PEDOT:PSSthin films deposited by spin and spray coating", Applied Surface Science, Vol. 338, pp 163-177, 2015.

[26] Xiong, K., Hou,L., Wu M., Huo Y., Mo W., Yuan, Y. et. al., "From spin coating to doctor blading : Asystematic study on the photo voltaic performance of an isoindigo-based polymer", Solar EnergyMaterials&SolarCells, Vol.132, pp. 252-259, 2015.

[27] Eggenhuisen T.M., Galagan, Y., Coenen, E.W.C., Voorthuijzen,W.P., Slaats, M.W.L., et. al., "Digital fabrication of organic solar cells by Ink jet printing using non-halogenated solvents", Solar EnergyMaterials&SolarCells, Vol. 134, pp. 364, 2015.

[28] J. Nelson, "Organic photovoltaic films", Curr. Opin. in Solid State Mat. Sci., Vol. 6, pp.87, 2002.

[29] Wallace G.G., et al., "Conjugated polymers: New materials for photovoltaics", Chemical Innovation, Vol. 30, pp. 14-22, 2000.

[30] Wikipedia, Polythiophene, 2014.
http://en.wikipedia.org/wiki/Polythiophene

[31] Ossila Limited, Regioregular poly(3-hexylthiophene-2,5-diyl), 2015.
http://www.ossila.com/oled_opv_ofet_catalogue3/PCDTBT_P3HT_PCBM_PED
OT_PSS_for_organic_photovoltaics/M101-P3HT.php

[32] Zhou, C., Liu, Z., Yan, Yushan D., X, Mai, Y-W., and Ringer S., "Electro-synthesis of novel nanostructured PEDOT films and their application as catalyst support", Nanoscale Research Letters, Vol. 6, pp. 364, 2011.

[33] Eslamian, M., Dashti, M., "Modeling spray coating and deposition of quantum-dot-sensitized nanoparticle thin film solar cells", 38th IEEE conference (Photovoltaics Specialists Conference), Austin, TX, 2012, pp. 2744–2749.

[34] Girotto, C., Moia, D., Rand, B.P., Heremans, P., "High-performance organic solarcells with spray coated hole-transport and active layers", Advanced Functional Materials Vol.21 pp. 64–72, 2011.

[35] Ishi, M., Narita, T., Hayata, Y., Nishimura, A., Tachi, K., "Simple and rapid fabrication of large-scale polymer-immobilized colloidal crystals by spray coating", Macromol. Mater. Eng., Vol. 296, pp. 687–692, 2011.

[36] Eslamian, M., "A mathematical model for the design and fabrication of polymersolar cells by spray coating", Drying Technol., Vol. 31, pp. 405–413, 2013.

[37] Xia, Y., Ouyang, J., "PEDOT:PSS films with significantly enhanced conductivities induced by preferential solvation with cosolvents and their application in polymer photovoltaic cells", J. Mater. Chem. Vol. 21, pp, 4927–4936, 2011.

[38] Björström, C., Bernasik, A., Rysz, J., Budkowski, A., Nilsson, S., Svensson, M., et al, "Multilayer formation in spin-coated thin films of low-bandgap polyfluorene: PCBM blends", Journal of Physics: Condensed Matter, Vol.17, 2005.

[39] Hummelen, J. C., Knight, B., W.; Lepeq, F., Wudl, F, Yao, J., Wilkins, C. L., "Preparation and Characterization of Fulleroid and Methanofullerene Derivatives", The Journal of Organic Chemistry, Vol. 60, pp. 532–538, 1995.

[40] Halls, J.J.M., Pichler, K., Friend, R.H., Friend, Moratti, S.C., and Holmes, A.B., "Exciton diffusion and dissociation in a poly(p-phenylenevinylene)/C60 heterojunction photovoltaic cell." Applied Physics Letters, vol. 68, pp. 3120–3122, 1996.

[41] Marks, R. N., Halls, J. J. M. , Bradley, D. D. C., Friend, R. H., Holmes, A. B., "The photovoltaic response in poly(p-phenylene vinylene) thin- film devices." Journal of Physics-Condensed Matter, Vol. 6, pp. 1379–1394, 1994.

[42] Peumans, P., Yakimov, A., Forrest, S.R., "Small molecular weight organic thin-film photodetectors and solar cells." Journal of Applied Physics, Vol. 93 pp. 3723, 2003.

[43] Weiran, C., Jiangeng, X., "Recent progress in organic photovoltaics: device architecture and optical design", Energy & Environmental Science, Vol.7, pp.2123, 2014.

[44] Heeger, M., Alan J. "Bulk Heterojunction Solar Cells: Understanding the Mechanism of Operation", Advanced Materials Vol. 26 pp.: 10–28, 2014.

[45] Wikipedia, Spin Coater , 2014.
https://en.wikipedia.org/wiki/Spin_coating

[46] National Nanotechnology Research Center UNAM, 2015.
http://unam.bilkent.edu.tr/?al_product=spinners

[47] OSSILA, Spin Coating Technique, 2015.
http://www.ossila.com/pages/spin-coating

[48] Geng, H. Semiconductor Manufacturing Handbook; McGraw-Hill: New York, 2004.

[49] Sigma Aldrich, PEDOT:PSS, 2014.
http://www.sigmaaldrich.com/materials-science/material-science-products.html?TablePage=113790002#sthash.ie7bNtV0.dpuf

[50] Zabihi ,F., Xie,Y., Gao, S., Eslamian,M., "Morphology, conductivity, and wetting characteristics of PEDOT:PSS thin films deposited by spin and spray coating", Applied Surface Science, Vol. 338, pp. 163-177, 2015.

[51] Dhritiman G., Sabyasachi, M., Narayan, K.S., "Fill factor in organic solar cells", Solar Energy Materials & Solar Cells, Vol. 94 pp. 1309-1313, 2010.

[52] Cappella, B., Dietler, G., "Force-distance curves by atomic force microscopy", Surface Science Reports, Vol. 34, pp. 1-3, 1999.

[53] Sze, S.M., Physics of Semiconductor Devices, 2nd ed., Wiley-Interscience, New York, 1981.

[54] Goetzberger, A., Knobloch, J., Voss, B., "Crystalline Silicon Solar Cells", Wiley, Newyork, 1998.

[55] Xue, J., Uchida, S., Rand, B.P., Forrest, S.R., "4.2% efficient organic photovoltaic cells with low series resistances", Appl. Phys. Lett. Vol. 84, pp. 3013-3015, 2004.

[56] Schilinsky, P., Waldauf, C., Brabec, C.J., "Recombination and loss analysis in polythiophene based bulk heterojunction photodetectors", Appl. Phys. Lett. Vol. 81, pp. 3885-3887, 2002.

[57] Derkacs, D., Lim, S.H., Matheu, P., Mar, W., Yu, E.T., "Improved performance of amorphous silicon solar cells via scattering from surface plasmon polaritons in nearby metallic nanoparticles", Appl. Phys. Lett., Vol. 89, pp. 093103-093113, 2006.

[58] Maier, Stefan A., Plasmonics: Fundamentals and Applications , Springer, New York, 2007.

[59] Bohren, C.F., Huffman, D.R., "Absorption and Scattering of Light by Small Particles.", Wiley, 2008.

[60] Mertz, J., "Radiative absorption, fluorescence, and scattering of a classical dipole near a lossless interface: a unified description.", J. Opt. Soc. Am. B Vol. 17, pp. 1906-19013, 2000.

[61] Andersson, V., Wuerfel, B., Uli, I, "Full day modeling of V-shaped organic solar cell.", Sol. Energy, Vol. 85, pp.1257-1263, 2011.

[62] Bohren, C. F., "How can a particle absorb more than the light incident on it". J. Phys. Vol. 51,pp 323-327, 1983.

[63] Catchpole, K.R., Polman, A., "Design principles for particle plasmon enhanced solar cells." Appl. Phys. Lett., Vol. 93,pp. 191113-191123, 2008.

[64] Wang, C.C.D., Choy, W.C.H., Duan, C., Fung, D.D.S., Sha, W.E.I., Xie, F.X., Huang, F., Cao, Y "Optical and electrical effects of gold nanoparticles in the active layer of polymer solar cells." J. Mater. Chem. Vol. 22, pp. 1206-1211. , 2012.

[65] Wu, J., Chen, F., Hsiao, Y., Chien, F., Chen, P., Kuo, C..et al.,"Surface plasmonic effects of metallic nanoparticles on the performance of polymer bulk heterojunction solar cells." ACS Nano, Vol. 5,pp. 959–967, 2011.

[66] Yang, G., Laser Ablation in Liquids Principles and Applications in the Preparation of Nanomaterials. Pan Stanford, 2012.

[67] Pillai, S., Catchpole, K.R., Trupke, T., Green, M.A., "Surface plasmon enhanced silicon solar cells." J. Appl. Phys., Vol. 101, pp. 093105- 93118, 2007.